THE DETECTION OF ELECTRICALLY-INDUCED SECONDARY FLOWS IN A PIPE BY MEANS OF ELECTROSTATIC PROBES

Henry R. Velkoff and Edwin R. Pejack

Department of Mechanical Engineering

The Ohio State University
Research Foundation
Columbus, Ohio

Technical Report No. 7

August, 1967

DISTRIBUTION OF THIS DOCUMENT IS UNLIMITED

DDC
RECEIVED
OCT 1 3 1967
C

55

THE DETECTION OF ELECTRICALLY-INDUCED SECONDARY FLOWS IN A PIPE BY MEANS OF ELECTROSTATIC PROBES

Henry R. Velkoff and Edwin R. Pejack

Department of Mechanical Engineering

The Ohio State University
Research Foundation
Columbus, Ohio

August, 1967

DISTRIBUTION OF THIS DOCUMENT IS UNLIMITED

FOREWORD

This report represents one phase of a general study of the interaction of ions with fluid flows under Contract DA-31-124-ARO-D-246, U. S. Army Research Office - Durham, with Dr. Henry R. Velkoff serving as principal investigator.

ABSTRACT

An experimental investigation was conducted to detect the presence of electrically induced secondary flows inside a round pipe. A thin concentric wire in the pipe was impressed with a high positive voltage which generated a corona discharge, producing ions and a radial electric field in the pipe. It was postulated that secondary flows taking the form of vortex flows inside the pipe would result.

A technique of utilizing electrostatic probes inserted into the pipe and on the wall provided strong evidence that secondary flows were generated both with and without a primary axial flow. At zero axial flow the characteristic length of the secondary flow was on the order of two pipe diameters. With an axial flow, when the primary and secondary flows are superimposed, various characteristic lengths were observed.

TABLE OF CONTENTS

LIST OF ILLUSTRATIONS

LIST OF SYMBOLS

E	electric field strength
f	friction factor
f_i	friction factor with ion current
J_p	probe current density
J_o	current density at $r = R$
k	positive ion mobility
K	Boltzmann's constant
n	ion number density
N	charge number from Eq. (11)
r	radius
R	inside radius of pipe, 0.75 inch
Rey	Reynolds number, $\frac{2Rv_m}{\nu}$
v	velocity
v_m	mean velocity
ϵ	dielectric premittivity
ν	kinematic viscosity
μ	viscosity
λ	wavelength

STATEMENT OF THE PROBLEM

References 1-3 reported significant increases in friction factor and velocity distribution in channel flow when an ion current was established transverse to the gas flow. As an ion source these investigations utilized a corona discharge from thin wires maintained at high voltage with respect to the channel walls; ions of one polarity drifted out of the corona sheath and across the gas stream while ions of the other polarity were present only in the thin corona sheath on the wires and drifted into the wire. Such configurations for a round and flat channel are shown in Fig. 1.

Table I below lists some of the results of the effect of the ion current on the main channel flow friction factor for laminar flow of air. It is seen that first-order effects are caused by the ion-fluid interaction.

Table I

Reference	Channel	J_0, $\mu A/inch^2$	f_i/f
1	$1\frac{1}{2}$ inch dia. pipe	0.94	1.76
2	$1\frac{1}{4}$ inch dia. pipe	1.77	1.75
3	5/8" x 5" duct	3.33	1.8

In Table I above

J_0 = ion current density at the channel wall,

f = friction factor for no current, and

f_i = friction factor with current.

A precise theory quantitatively expressing the effect of the transverse ion current on the axial channel flow has not yet been developed; in fact, the mechanism for interaction has not been definitely established. Reference 1 hypothesizes that the corona sheath surrounding the wires directly affects the mean flow through viscous action; reference 2 postulated the existence of a flow-induced electric field which results in an upstream-directed body force on the mean flow. Reference 4 considered that transverse electric forces could destabilize the mean flow and superimpose electrically induced secondary vortex flows. Such secondary flows would then provide a transport mechanism resembling a large-scale
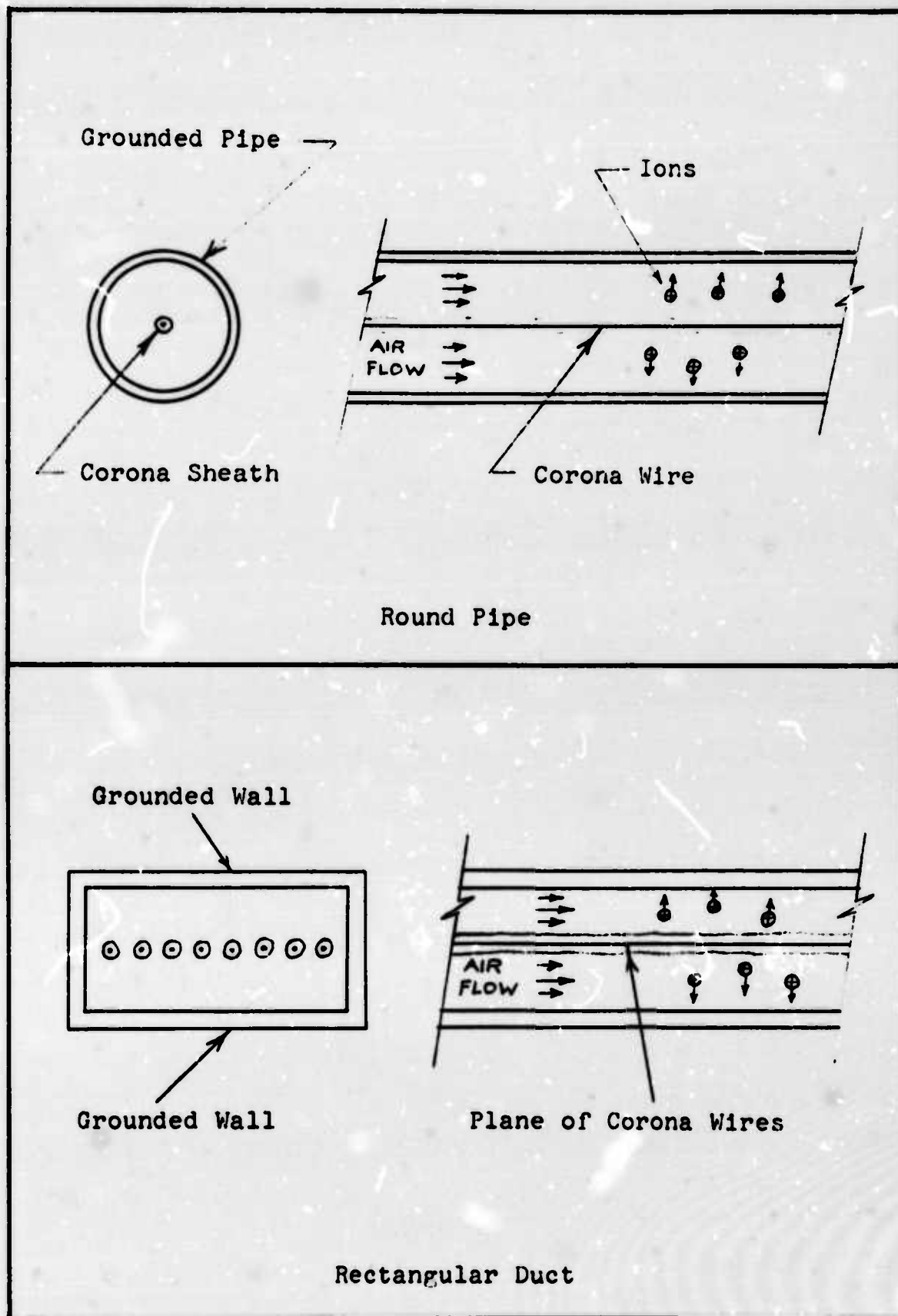
1

Fig. 1 Typical flow channels with corona

2

turbulence which would increase the axial flow friction factor and change the velocity distribution.

The concern of the present investigation is to experimentally detect the existence of electrically induced secondary flows by means of electrostatic probes.

An electrostatic probe is an electrically conducting surface which is inserted into a region of ionized gas and through collisions of ions on the probe surface draws a current in the electric circuit connected to the probe. If different values of potential are impressed on the probe by the probe circuit, then the probe current will be affected and consequently a probe current-probe voltage curve or characteristic is obtained. If the probe itself does not significantly change the properties of the ionized gas, then from the probe characteristic the number density of ions and the potential of the ionized gas at the location of the probe can be calculated.

DESCRIPTION OF THE FLOW CHANNEL AND ELECTROSTATIC PROBES

The flow channel used in the present report was 1.5-inch inside diameter round pipe 136 inches long. A 0.004-inch diameter steel wire was stretched taut along the centerline and insulated from the pipe walls. At a point 115 inches downstream from one end of the pipe a 1/8-inch diameter brass rod probe was inserted 1/8 inch into the pipe along a radius. The sides of this rod were covered with a covering of 1/16-inch thick nylon, so only the end of the rod surface contacted the gas in the pipe. One-half inch further downstream was a similarly placed rod probe identical to the one above. The end surfaces of these two rods served as electrostatic probe surfaces and will hereafter be referred to as the rod probes. A sketch of the rod probes is shown in Fig. 2.

A section of the pipe beginning approximately 120 inches downstream from the end of the pipe was constructed of a series of thirty 3/32-inch wide rings, each separated electrically by an 0.004-inch thick intervening sheet of vinyl plastic. Each ring had a pin imbedded in its outside diameter to serve as an electrical connector, and the entire set of rings were cemented together and positioned in line with the rest of the pipe (see Fig. 2). There were 30 rings in all, numbered consecutively from the downstream ring to the upstream ring. The inside surface of any ring of course was exposed to the gas in the pipe and, therefore, could be used as an electrostatic probe whose position is at the radius R of the pipe.

Air was supplied to the flow channel from the laboratory compressed air supply, as shown in Fig. 3. The downstream end of the pipe exhausted into the atmosphere. The central corona wire was connected to a high-voltage power supply; the pipe itself (aluminum) was electrically grounded.
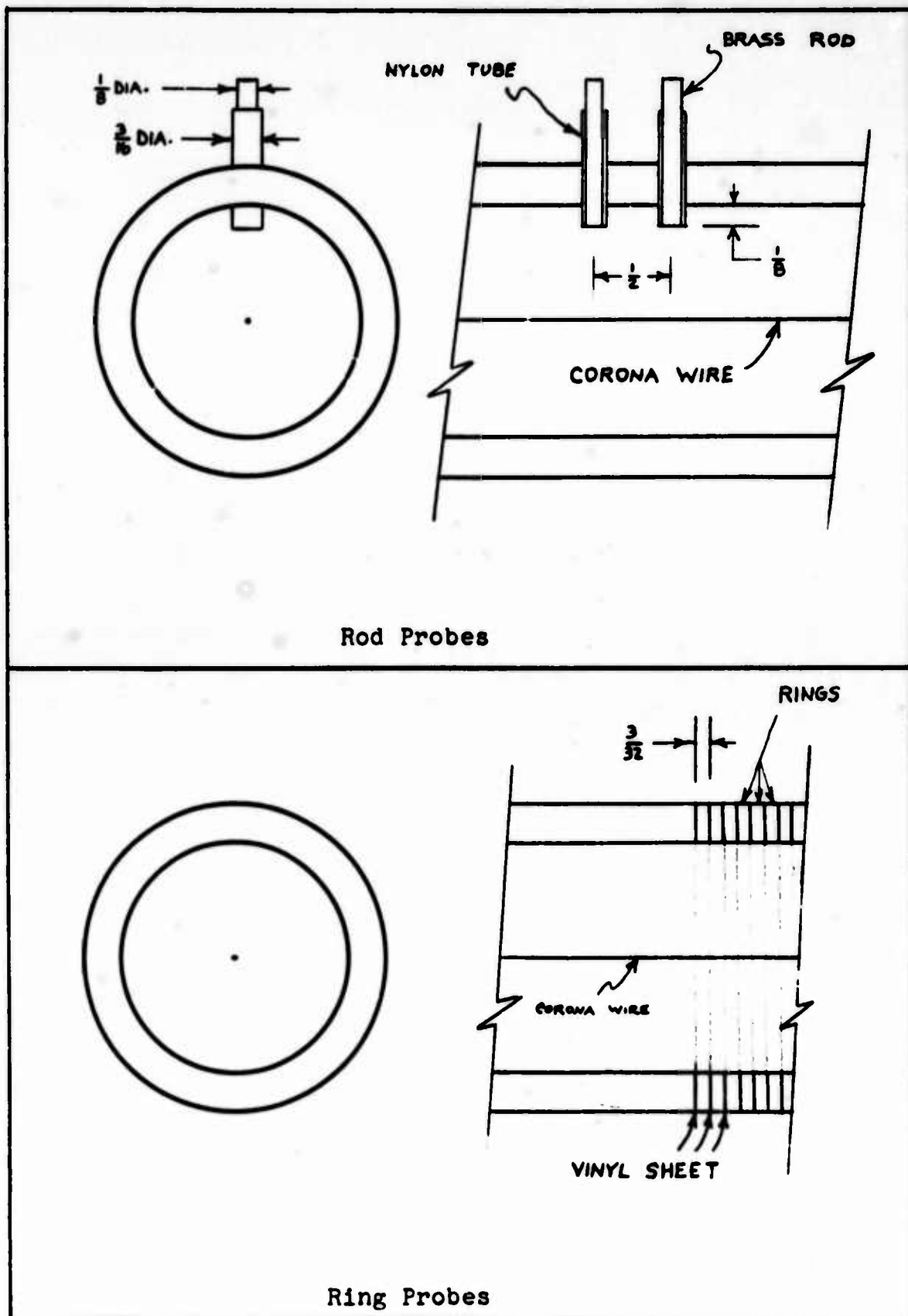
3

Fig. 2 Electrostatic Probes

4

Fig. 3 Flow Diagram

5
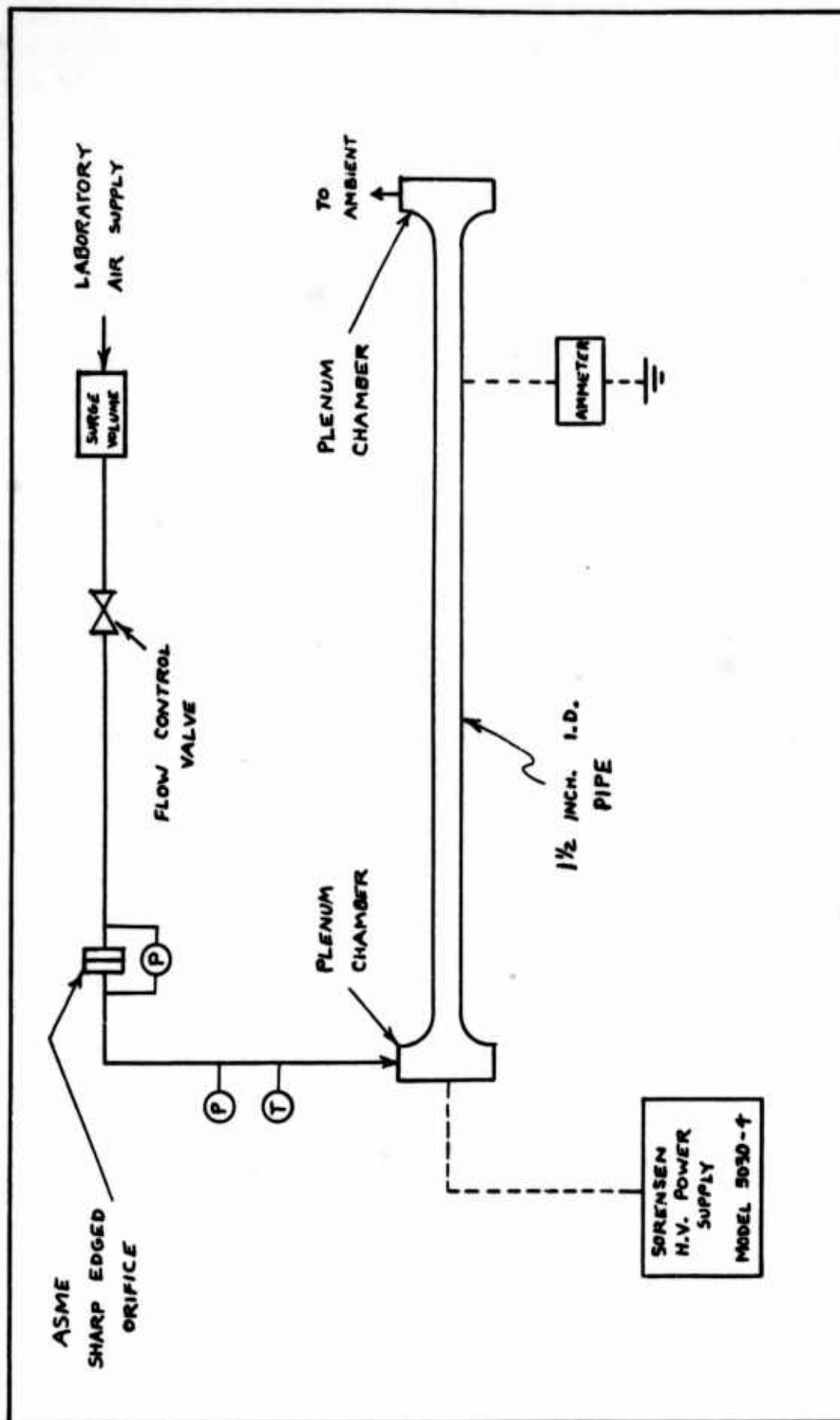
ELECTROSTATIC EQUATIONS

The electric field equations are assumed to one-dimensional; i.e., no component of field strength exists in the axial direction. Using Maxwell's equation

$$\vec{\nabla} \cdot \vec{E} = \frac{n}{\epsilon} \tag{1}$$

or

$$\frac{1}{r} \frac{d(Er)}{dr} = \frac{n}{\epsilon} . \tag{2}$$

The local current density J is given by

$$J = nkE , \tag{3}$$

where

n is the number of density of positive ions,

k is the ion mobility, and

E is the local value of field strength.

From current continuity

$$Jr = J_oR \tag{4}$$

where subscript o represents values at the pipe wall, r = R. Equation (2) then reduces to

$$(Er)d(Er) = \frac{J_oR}{k\epsilon} r . \tag{5}$$

Integrating,

$$(Er)^2 = \frac{J_oR}{k\epsilon} r^2 + \text{constant.} \tag{6}$$

6

A space-charged limited condition is assumed at the edge of the corona sheath at $r = r_1$. Therefore, $E = 0$ at $r = r_1$. Equation (6) yields

$$(Er)^2 = \frac{J_0 R}{k\epsilon} [r^2 - r_1^2] ; \qquad (7)$$

but the corona sheath radius r_1 is small compared to the radius r for most of the pipe, so Eq. (7) is written approximately as

$$E = \left[\frac{J_0 R}{k\epsilon}\right]^{1/2} . \qquad (8)$$

The ion density n, using Eq. (3), (4), and (8), can be written

$$n = \left[\frac{J_0 R \epsilon}{k r^2}\right]^{1/2} . \qquad (9)$$

Equation (9) can be averaged over the pipe volume to find an average ion density $\bar{n}$:

$$\bar{n} = \left[\frac{4 J_0 \epsilon}{Rk}\right]^{1/2} . \qquad (10)$$

Following reference 2 a nondimensional group, called a charge number, is defined as

$$N = \frac{\bar{n} R^2}{\mu k} = \left[\frac{4 J_0 \epsilon}{Rk}\right]^{1/2} \frac{R^2}{\mu k} .$$

For the flow channel in this report the charge number as a function of current density J_0 on the pipe wall is given by Table II, where a positive ion mobility of 0.216 inch^2 volt^{-1} sec^{-1} was assumed.[5]

Table II

Charge Number N	Current Density $\mu A/inch^2$
2	0.00963
5	0.0602
10	0.241
15	0.542

7

The charge number N was found in Ref. 2 and 3 to be a convenient parameter for correlating the ion current effect on the friction factor. For example, in the present case the static pressure drop between two pressure taps at 45 inches and 127 inches from the upstream end of the channel, and the friction factor were calculated. In laminar flow, the friction factor at a constant charge number is seen to possess a laminar characteristic, as shown in Fig. 4. Also, the group f_i Rey is found to be linear with the charge number, as shown in Fig. 5. These results agree with the findings reported in Ref. 2 and 3.

MEASUREMENT OF ION DENSITY

The probe circuit shown in Fig. 6 was first connected to the upstream rod probe. The potential of the probe was varied by adjusting the variable resistors shown in Fig. 6. For no corona discharge in the pipe, the measured current due to leakage was very small and on the order of 0.003μ A at a probe potential of 400 V relative to the pipe wall. A corona discharge was then generated on the axial corona wire and the corona current set a value corresponding to a current density of 0.41 μA per square inch on the pipe wall. From Eq. (11) this corresponds to a charge number of 13.05, well within the region of significant ion-fluid interaction as seen from Fig. 5. With this value of charge number the probe characteristic was obtained for an axial flow Reynolds number of 0, 1270, and 3400 and is shown in Fig. 7. During this test the charge number varied less than 1% because of slight drift in the value of the corona current.

At high positive values of probe voltage the probe repels the positive charges and the probe current is low. Under this condition the gas near the probe surface is partially depleted of positive ions as compared to the undisturbed ion density. At high negative values of probe voltage, the probe begins to attract all ions in the vicinity of the probe and the current tends to level off to a high value.

If it is assumed that all ions which strike the probe are measured as current, that the ions possess a translational temperature very near the gas temperature, and that the velocity distribution is Maxwell-Boltzmann, then the ion density can be calculated from Fig. 7.[5] At a point on the probe characteristic corresponding to the knee of the curve, the probe is at a potential equal to the space potential of the ion gas at that point. Under this condition the probe neither attracts nor repels ions and the probe current J_p is related to the local ion density by the equation given in Ref. 5, page 140.

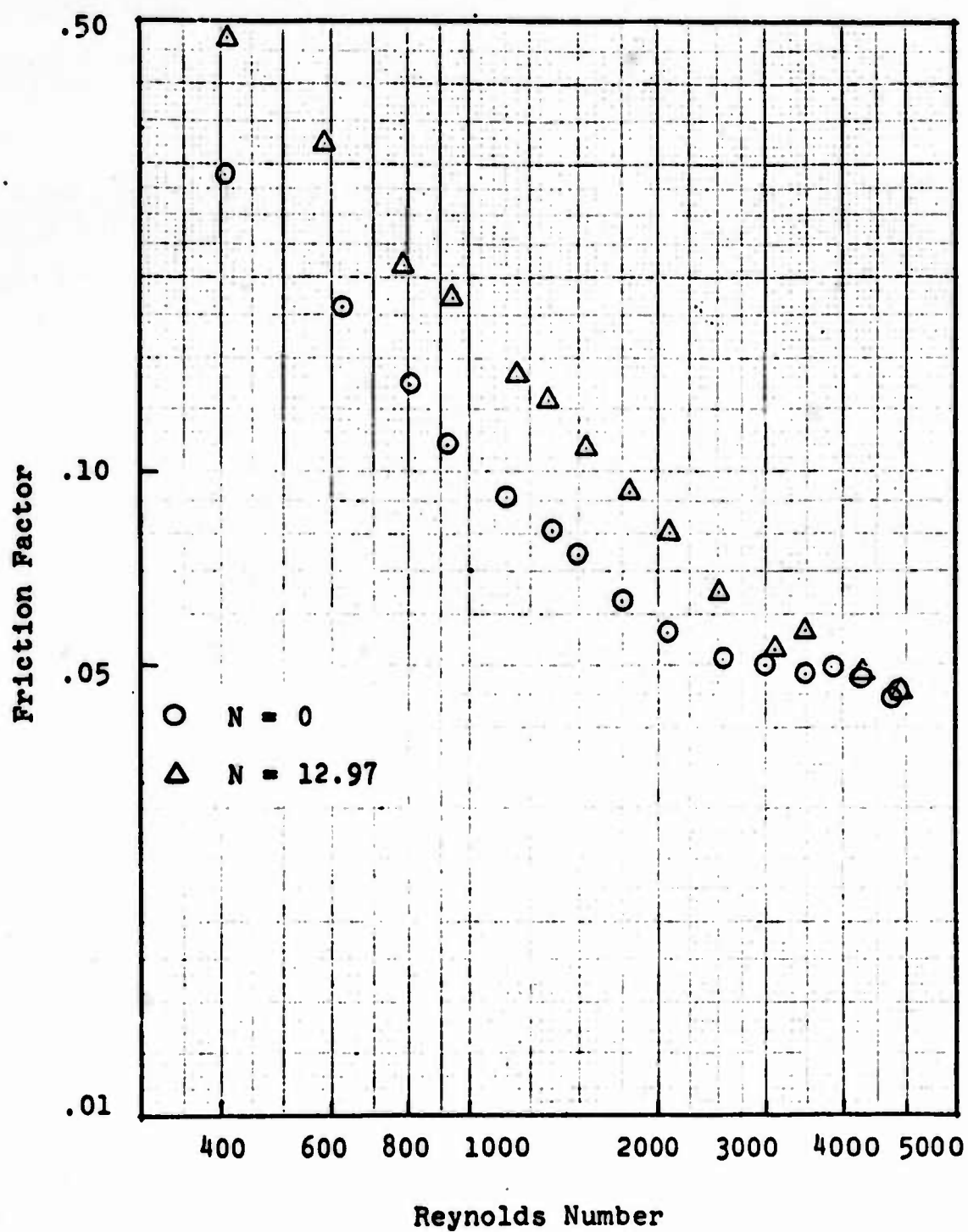$$n = 4J_p \left[\frac{\pi m}{8KT} \right]^{1/2} , \tag{12}$$

8

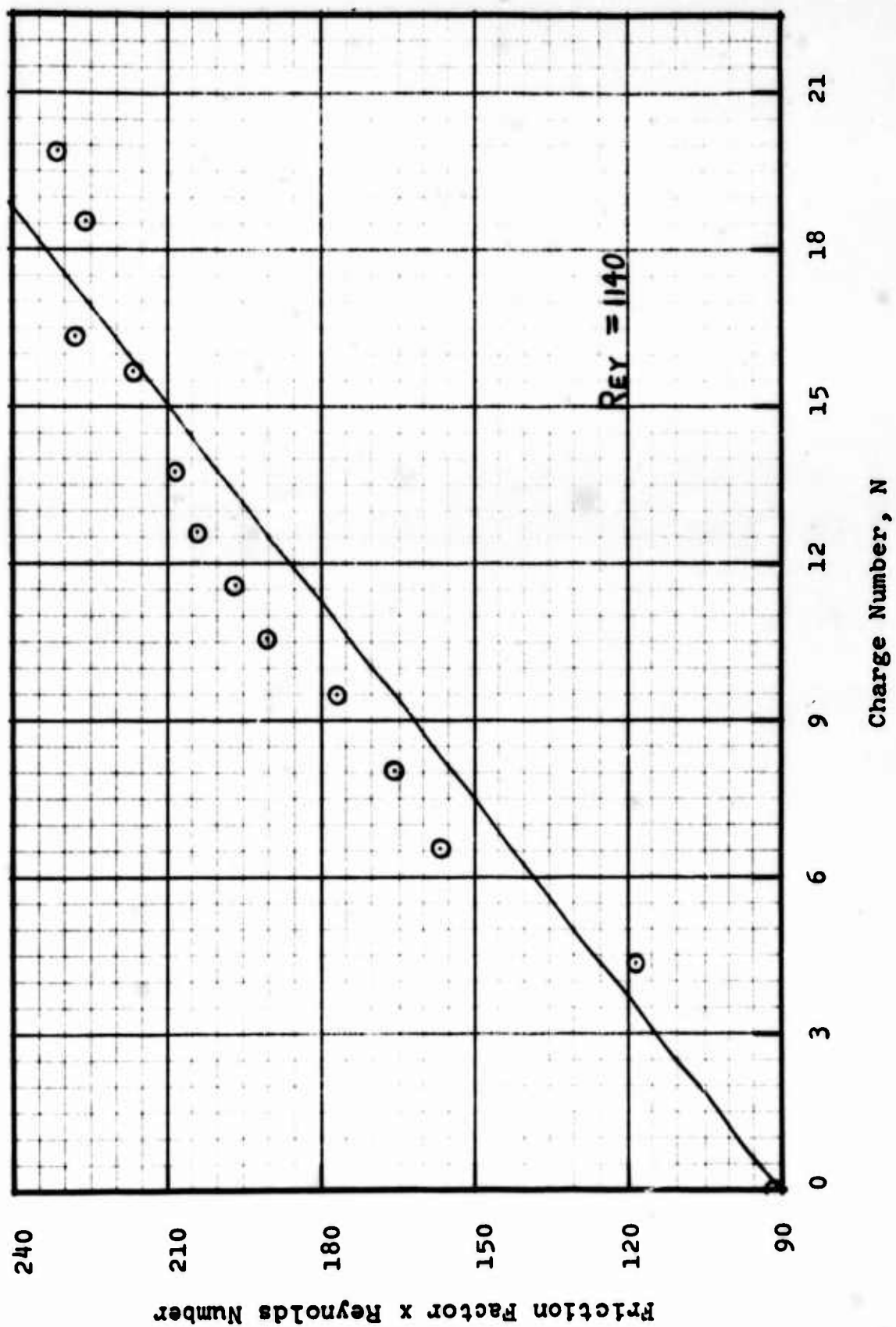Fig. 4   Log Friction Factor Versus Reynolds Number

9

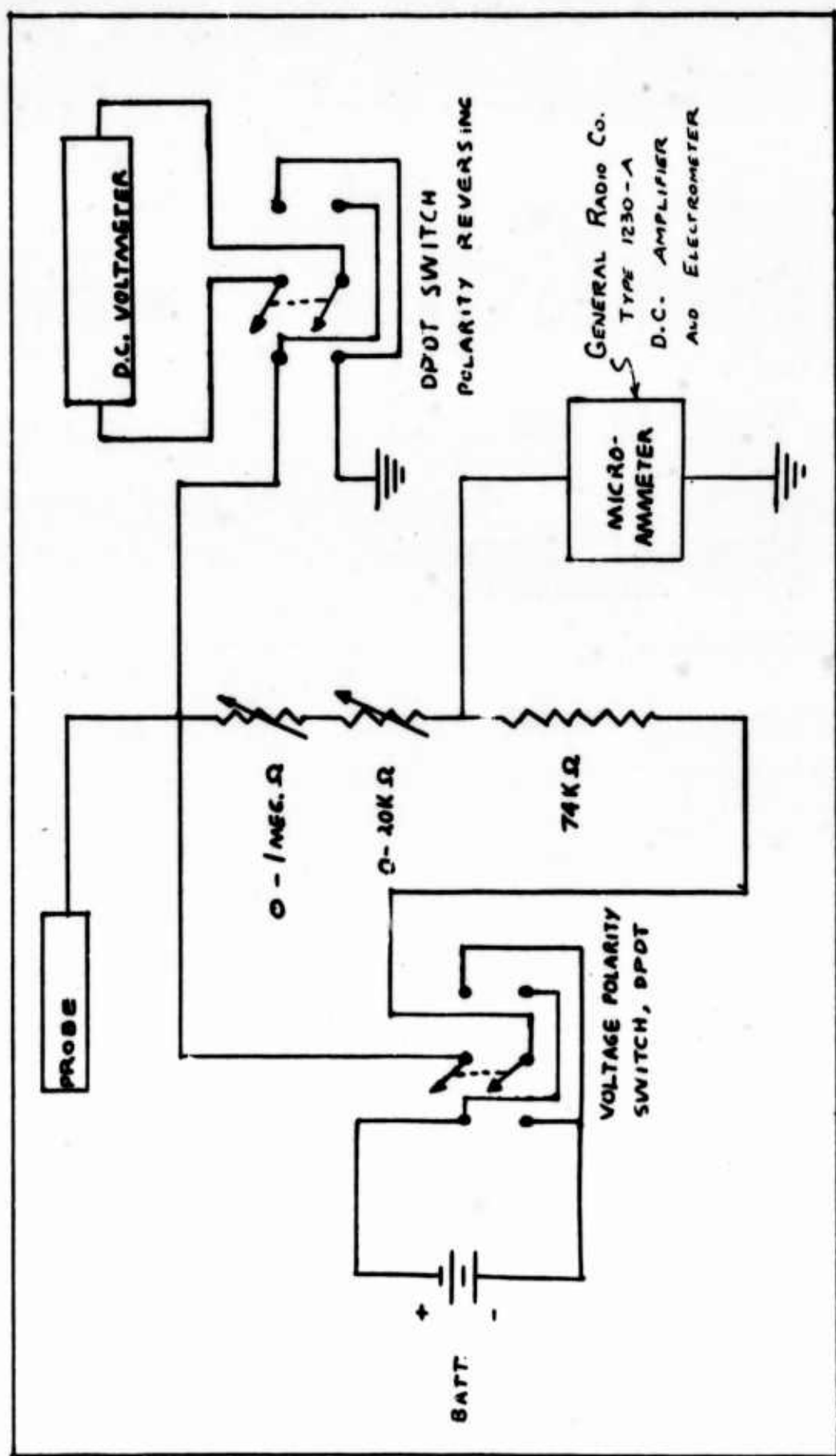Fig. 5   Friction Factor Times Reynolds Number Versus Charge Number
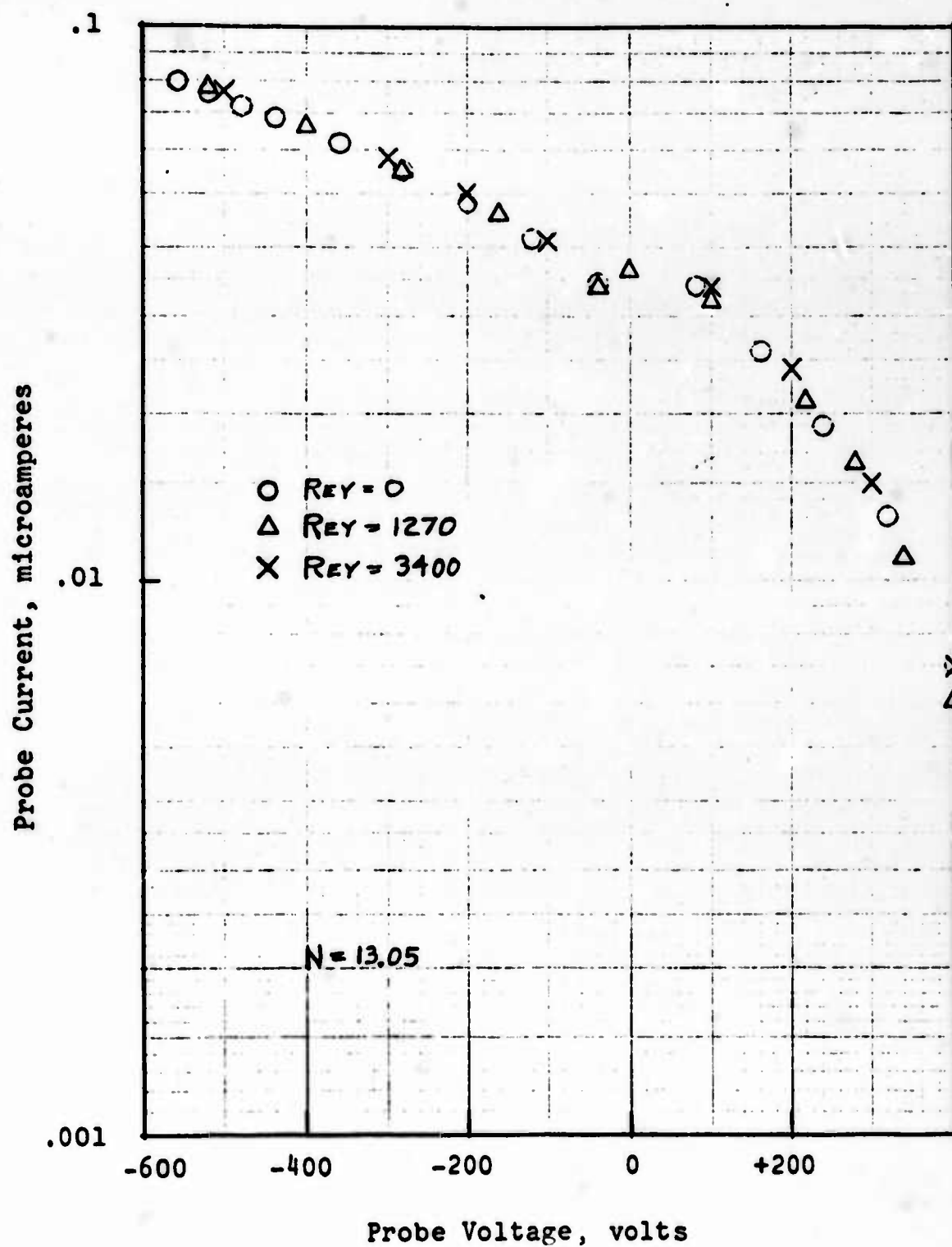
10

Fig. 6   Electrostatic probe circuit

11

Fig. 7   Probe Characteristic for Rod Probe

12

where

> m is the mass of the ion,
>
> T is temperature, and
>
> K is Boltzmann's constant.

Since the knee of the curve is not well defined, the probe current density can only be determined within about a factor of 10. For Fig. 7 the knee is at approximately a probe voltage of 250.

The three sets of points on Fig. 7 for different axial flow Reynolds numbers apparently fall on the same curve. There is, therefore, no indication that the mean axial flow of air has any effect on the local field strength or ion density at the point of the probe. This conclusion is further supported by Fig. 8 which shows the change in probe current with Reynolds number for a fixed probe voltage of 240. No significant change in probe current is observed as the Reynolds number is varied, except for a very small increase near a Reynolds number of zero.

Ring number 15 was also used as an electrostatic probe, with all the other rings grounded. In this case, as the probe voltage was changed relative to ground, the leakage current was measured as a function of probe voltage (see Fig. 9). A corona current was generated in the pipe corresponding to a charge number of 18.3 and the probe current measured as a function of the probe voltage. The measured probe currents were then corrected for leakage (see Fig. 9), and the net probe current plotted against the probe voltage as shown in Fig. 10. In this case the probe is at the outer radius R and the space potential should therefore be a a value of zero. The zero probe voltage point on Fig. 10 is with the portion of the curve constituting the knee, as expected. An almost identical curve was obtained for three Reynolds numbers of 0, 1260, and 3400, again indicating, as with the rod probe, that the ion density is not measurably changed by the mean air flow. This is similarly shown by a plot of the probe current versus Reynolds number at a constant probe voltage (Fig. 11). No large changes in J_p are observed as the Reynolds number is varied up to a value of 5000.

The ion density was calculated from the probe characteristics and Eq. (12) and was compared with the theoretical value from Eq. (9). The results for the rod and ring probes are shown in Table III. A temperature of 70°F and a mobility of 0.216 $inch^2$ $volt^{-1}$ sec^{-1} were used in the calculations. This value is representative of the mobility of the positive ion in air as given by Ref. 5, page 38.

The measured ion density values in Table II indicate reasonable agreement with the values predicted by Eq. (9). In particular it is noted that the level of ion density is very low compared to the number density of neutral molecules; i.e., on the order of one to 10.[11]
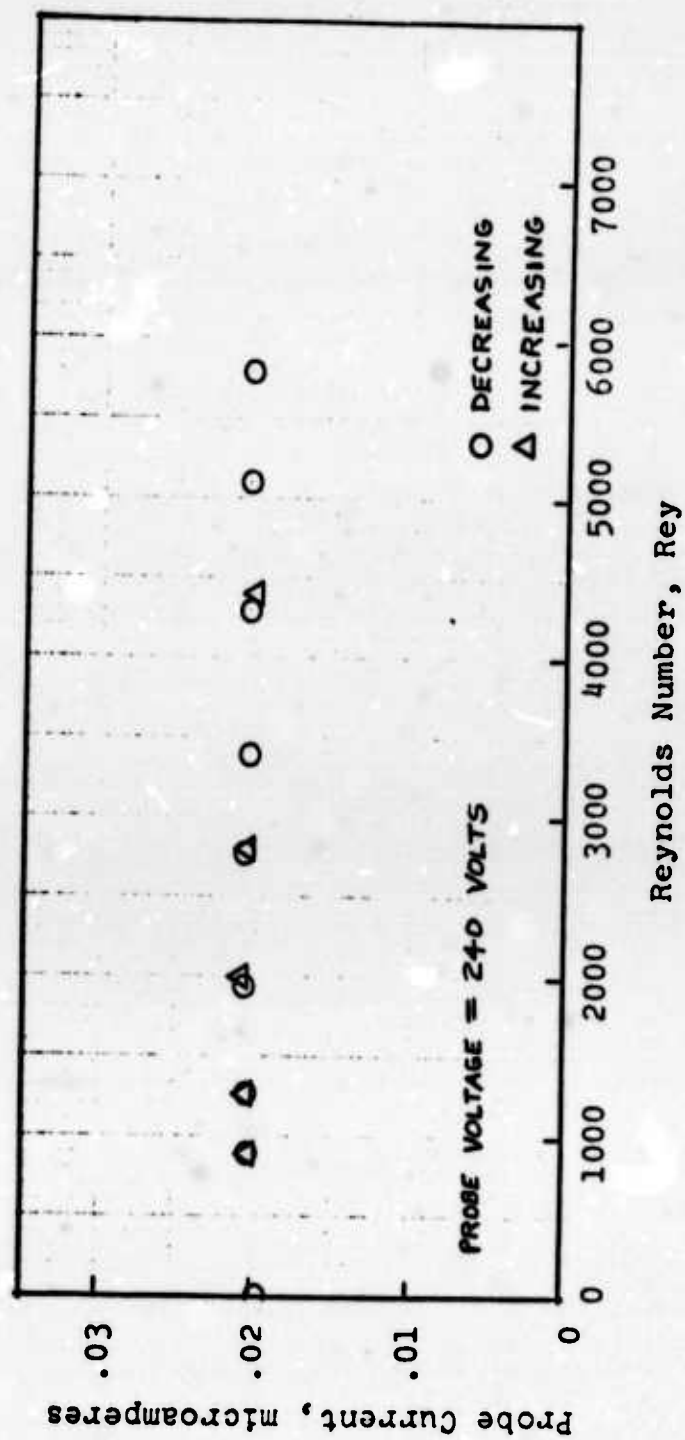
Fig. 8 Probe Current Versus Reynolds Number, rod probe
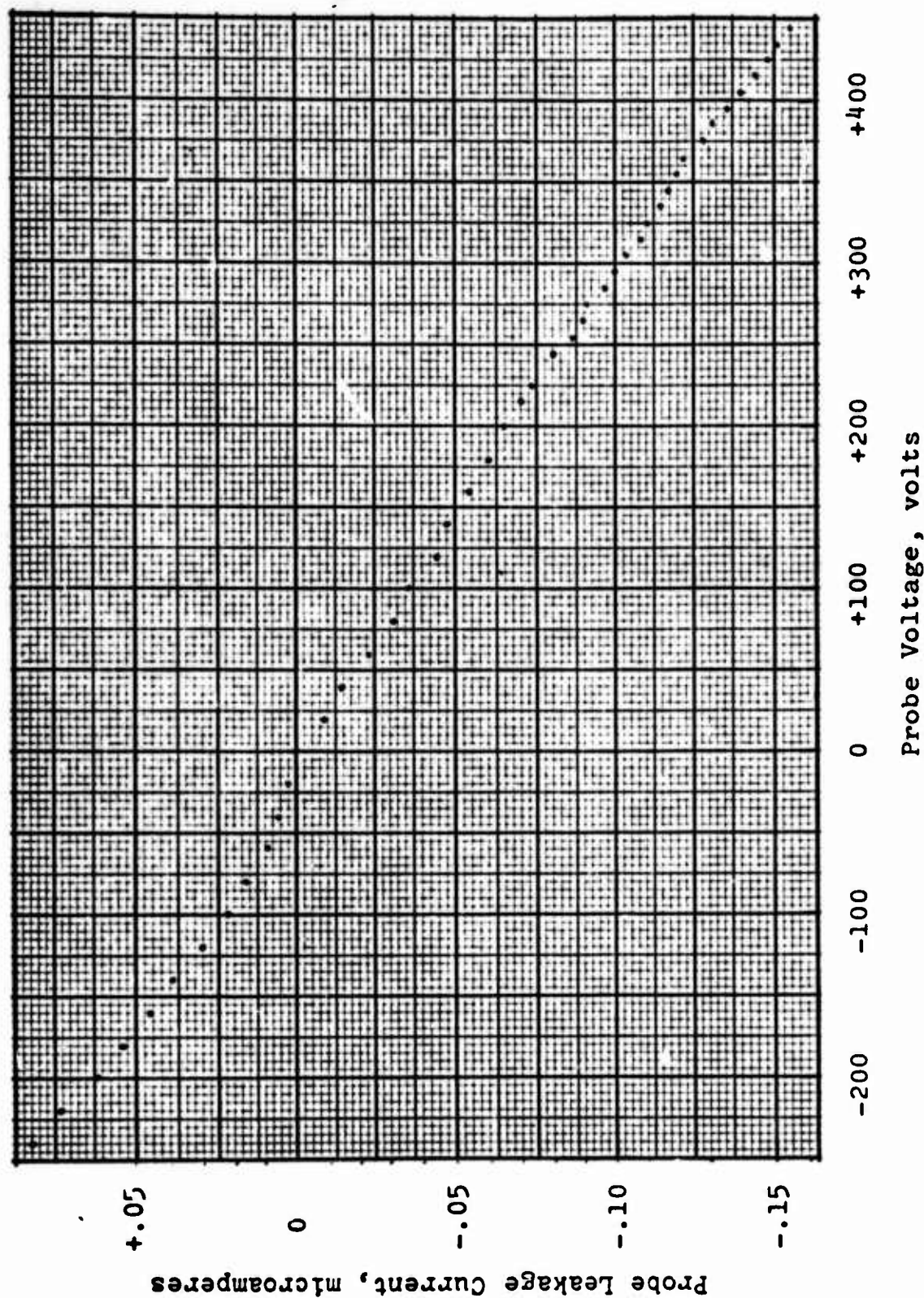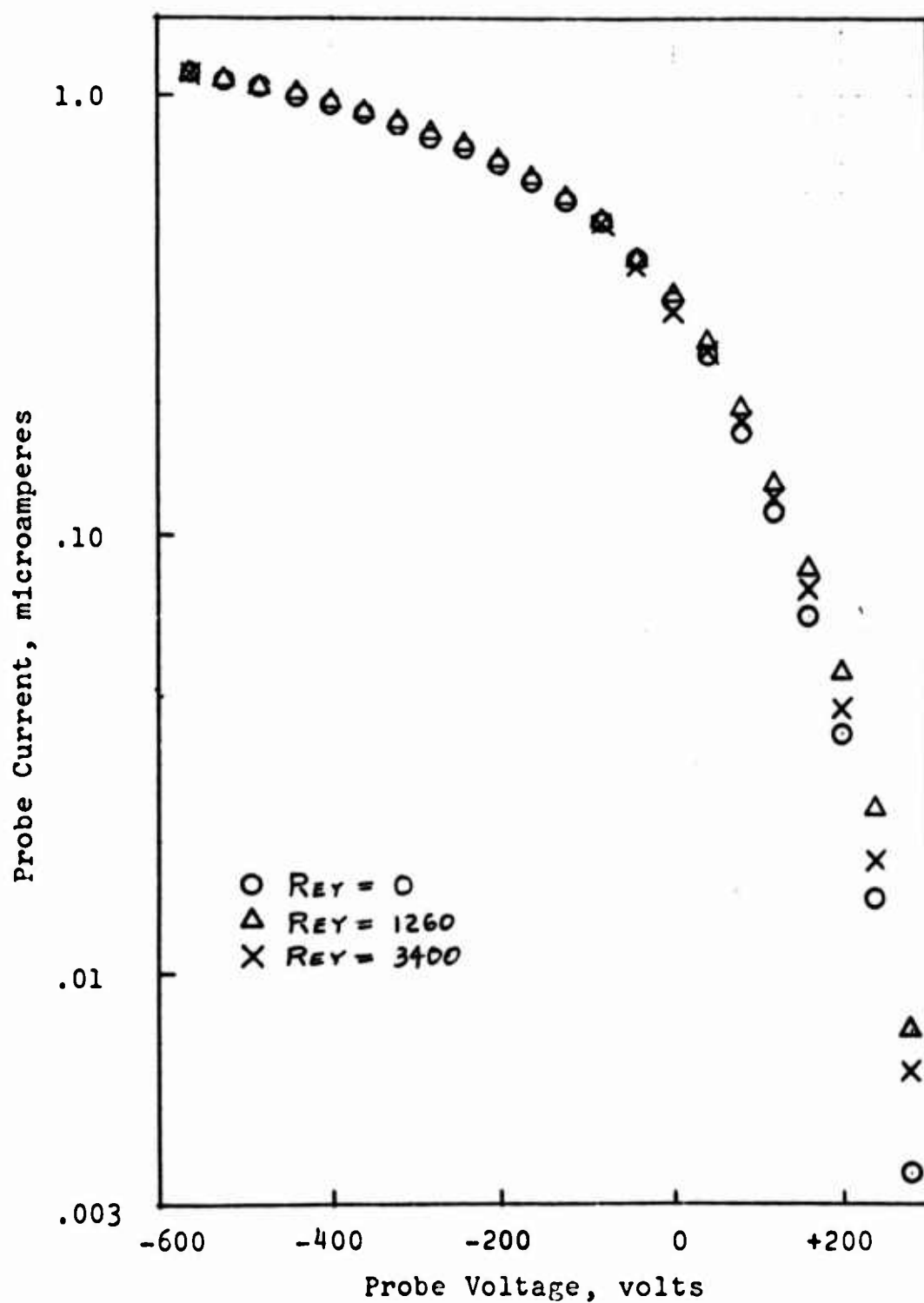
14

Fig. 9   Current Leakage for Ring Probe

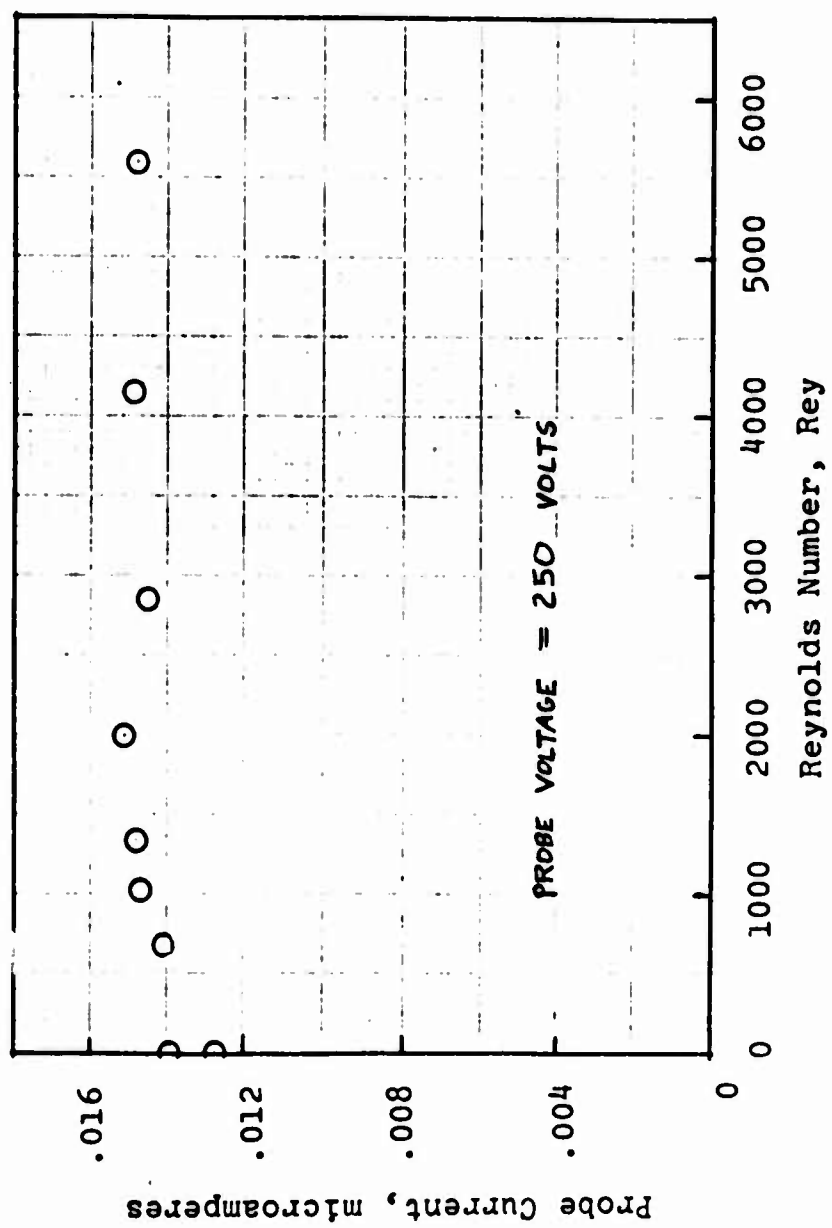Fig. 10   Probe Characteristic for Ring Probe, N = 18.3

16

Fig. 11 Probe Current Versus Reynolds Number, ring probe

17

Table III. Ion Density

| N | Current Density J_0 $\mu A/\text{inch}^2$ | Ion Density, Ions/inch^3 | | |
		Eq. (9)	Rod Probe	Ring Probe
18.3	.80	6.6×10^9	---	1×10^9
13.05	.41	5.6×10^9	2×10^9	---

MEASUREMENT OF MOVING DISTURBANCES

1. Rod Probe

The radial current density J results in a body force per unit volume in the radial direction. The equations of motion admit a solution such that no radial velocity component exists and a steady radial pressure gradient J/k is present. It is hypothesized, however, that the primary flow is unstable, and a secondary flow consisting of a toroidal vortex pattern (as in Fig. 12) will be superimposed on the primary flow. The secondary and the primary flows will in general combine in a complicated way.

A method for detecting the presence of the secondary flow results from the following reasoning:

When the primary flow is zero axial motion, the only motion present is the secondary flow. This type of flow has an analogy with the case of fluid between concentric cylinders with the inner cylinder rotating. The secondary flow in that case[6] was found to be toroidal vortices with a diameter equal to twice the width of the annulus. If in the present case a similar pattern of vortices is generated at zero primary flow, then an observer moving along the pipe at velocity v would encounter variable velocities with a periodicity λ/v, where λ is the wavelength. It is now assumed that if the primary flow is not zero, the combination of the primary and secondary flow will be such that a periodicity in the resultant flow will be maintained. Under this condition a stationary observer in the pipe will experience a periodic disturbance in velocity with a period λ/v, where v is now the velocity of the resultant flow and λ is the wavelength. This is akin to saying that the primary flow carries the secondary flow downstream.

The velocities associated with the secondary flow are expected to be very small and not detectable by ordinary means. However, by looking at the secondary flow pattern in Fig. 12, it is seen that as the pattern is moved past a stationary observer, the velocity will alternately add and detract from the radial drift velocity of the ions.
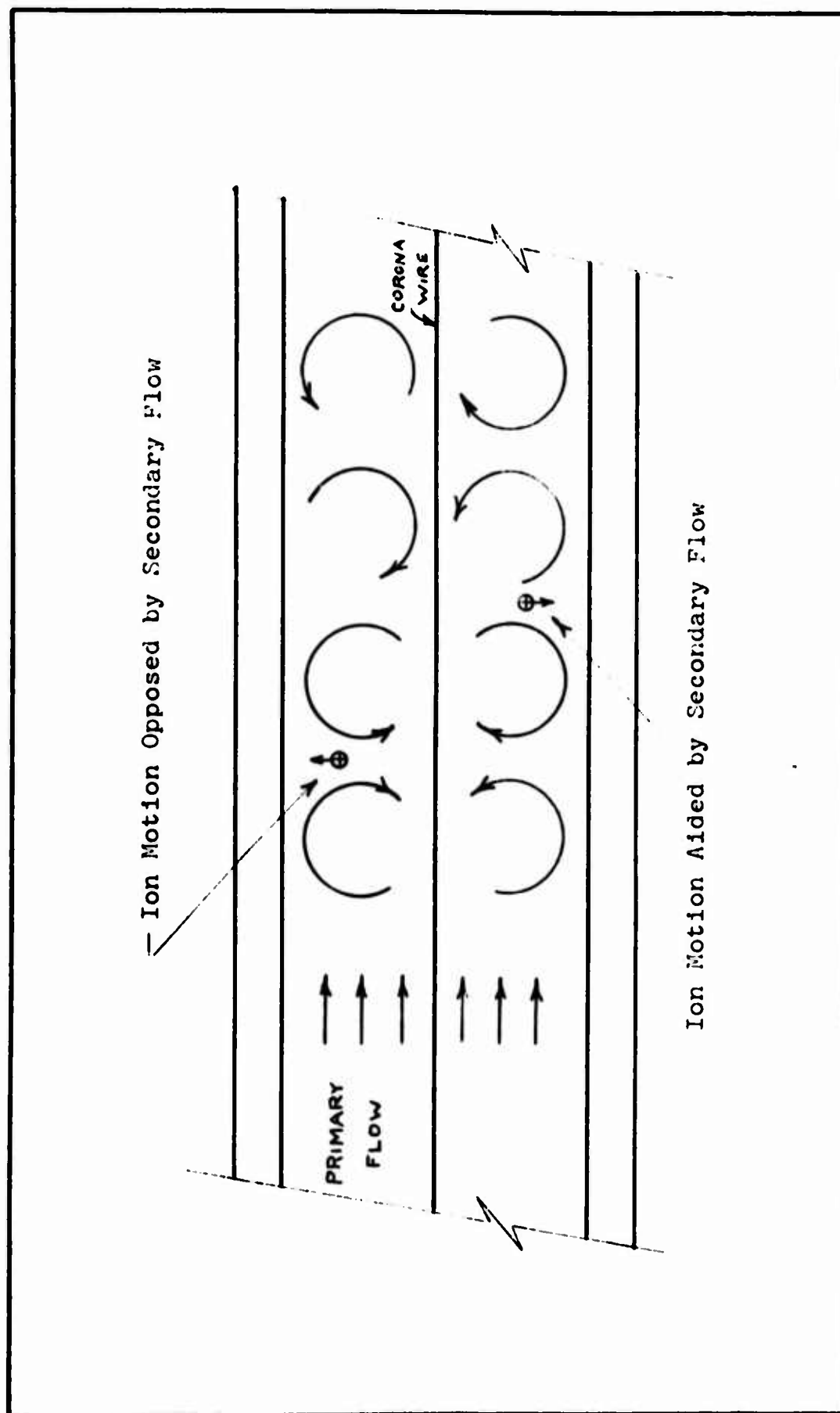
Fig. 12 Sketch of Induced Vortex Flow

19

Such an occurrence would impart a periodicity to the local ion density and current at the observer's position.

The two rod probes (Fig. 2) were therefore connected to the terminals of an oscilloscope. If no secondary flow were present it would be expected that no pattern would be detected on the scope; however, if secondary flows were present, from the previous reasoning a periodic disturbance would be detected. Figures 13-18 show the resulting oscilloscope traces for various Reynolds numbers from 0 to 1780 for a charge number 12.75. Photographs which show two traces merely indicate that two sweeps were made on the same film. From these traces the following observations are made: For zero flow, a slight periodic disturbance is measured; as the Reynolds number is increased, the amplitude of the distrubances increases to maximum values in the range of 600 to 900 Reynolds number and then decrease again to small relatively constant amplitudes above a Reynolds number of 1330.

The time-dependency of the traces reveals that the disturbances are not regular; however, certain recurring wavelengths are observed. It was anticipated that the moving disturbances would have a wavelength equal to the pipe diameter and move with the bulk fluid at a velocity equal to the mean velocity of the fluid. Therefore, the following length was calculated

$$\frac{\text{(Pipe Diameter)(Sweep Speed)}}{\text{(Mean Velocity)}}$$

and appears as a length indicated on each photograph. This distance is the horizontal length on the scope screen which corresponds to moving disturbances with a characteristic length equal to one pipe diameter. From the scope traces it is seen that the distance between sucessive relative maxima on the traces frequently does approximately equal the pipe diameter. This fact indicates that disturbances with a wavelength of one pipe diameter are moving down the pipe. It is also noticed that waves with longer and shorter lengths are also present.

Above a Reynolds number of about 1150 the disturbance pattern is seen to begin to posses a high-frequency component, which also is accompanied by a decrease and finally a leveling off of the amplitude. It may be that in this range of flow the secondary flow and the primary flow combine in a different way, and the relatively more regular pattern at low Reynolds numbers is lost. It may also be suspected that transition to true turbulence begins in this range; however, Fig. 4 indicates that the friction factor exhibits a laminar characteristic up to a Reynolds number of more than 2000. It is also noted that the friction factor curve of Fig. 4 did not seem to experience any change in trends at any Reynolds number below the transition Reynolds number at about 2500. Another possibility is that beginning at Reynolds numbers of about 1150,
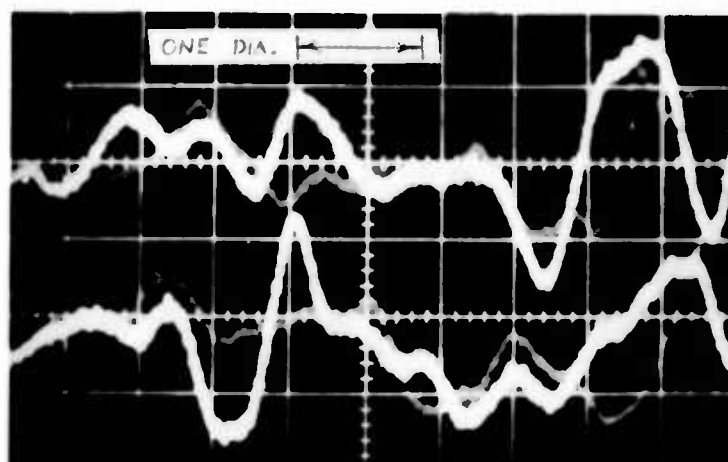
20
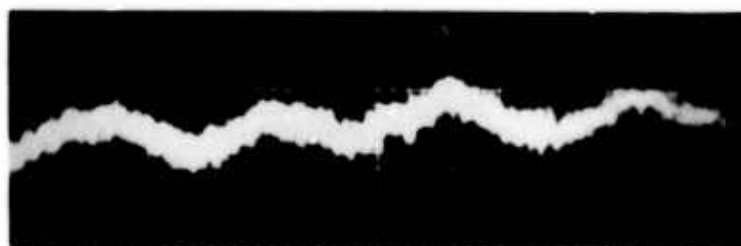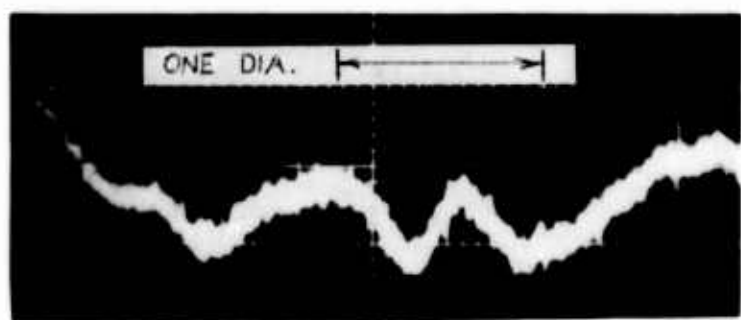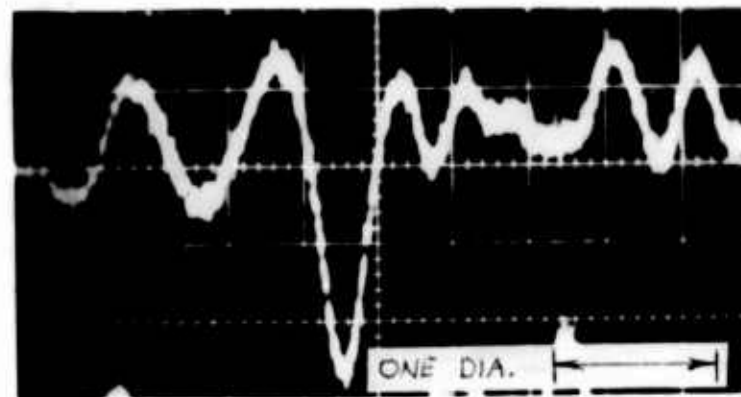
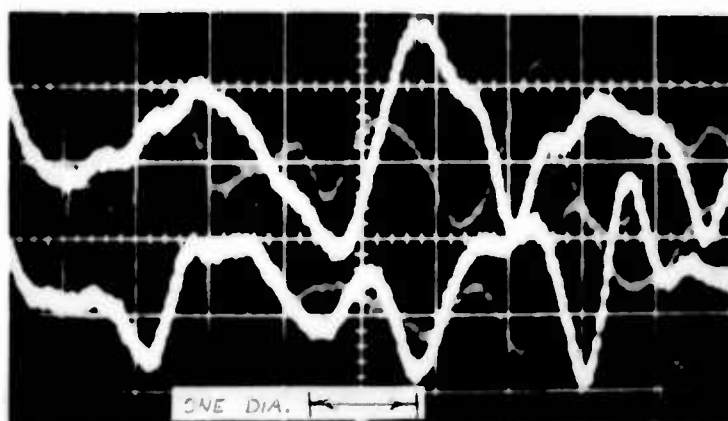Fig. 13   Fluctuations Between Rod Probes

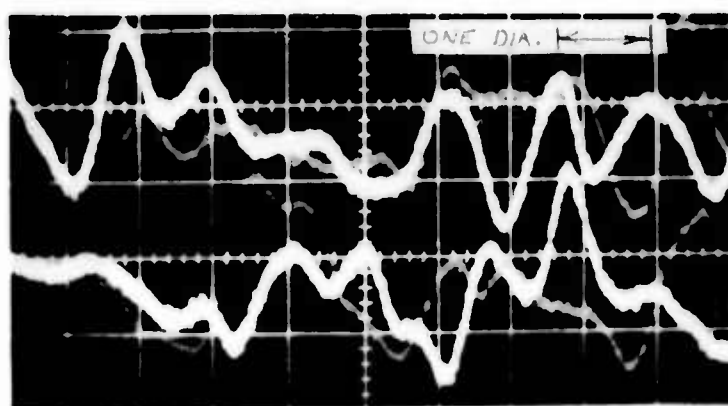N = 12.75; Sweep = 0.1 sec/cm; Amplitude = 1 mv/cm

21

Fig. 14   Fluctuations Between Rod Probes

N = 12.75; Sweep = 0.1 sec/cm; Amplitude = 2 mv/cm

22

Rey = 770

Rey = 850

Rey = 950

Fig. 15   Fluctuations Between Rod Probes

N = 12.75; Sweep = 0.1 sec/cm; Amplitude = 2 mv/cm

23

Rey = 1050
Amplitude = 2 mv/cm
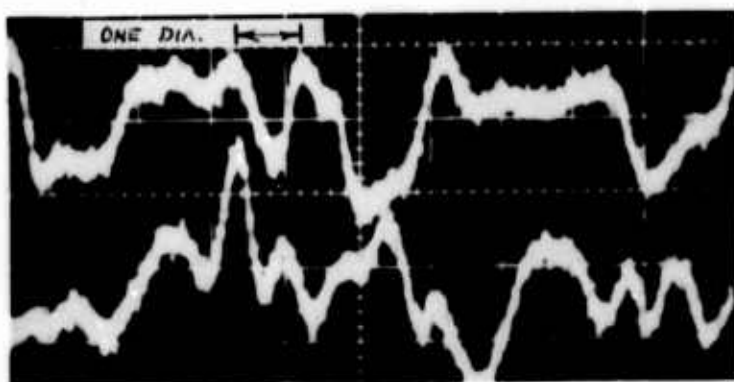
Rey = 1050
Amplitude = 1 mv/cm
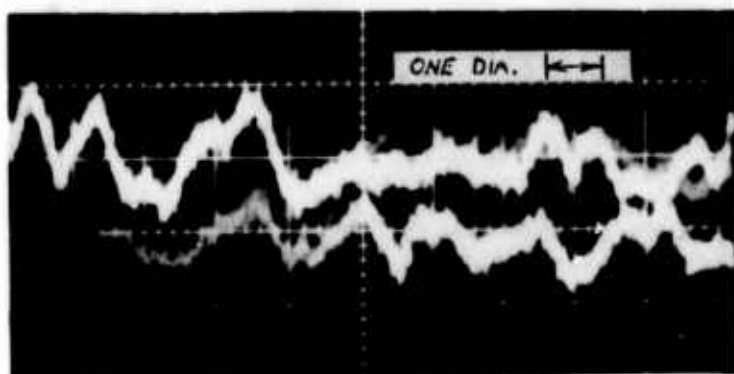
Rey = 1150
Amplitude = 1 mv/cm

Fig. 16   Fluctuations Between Rod Probes

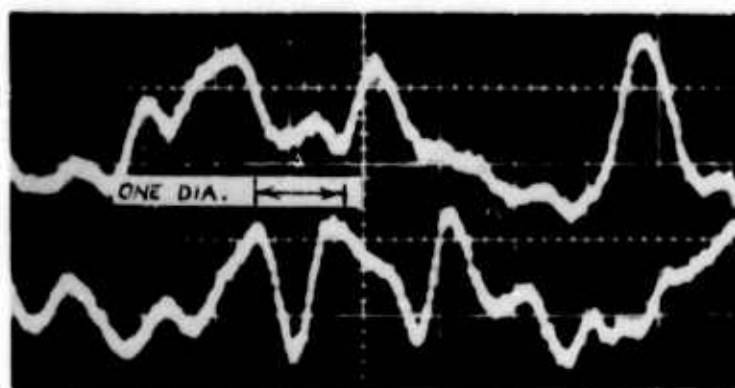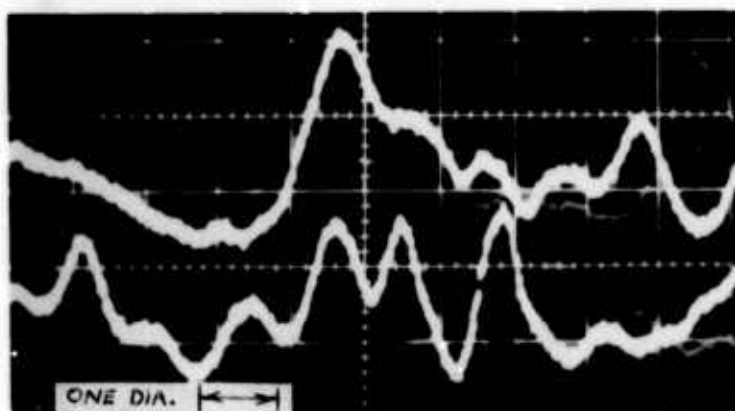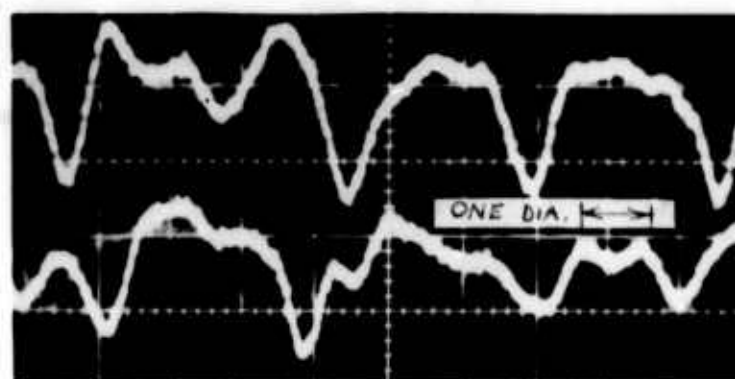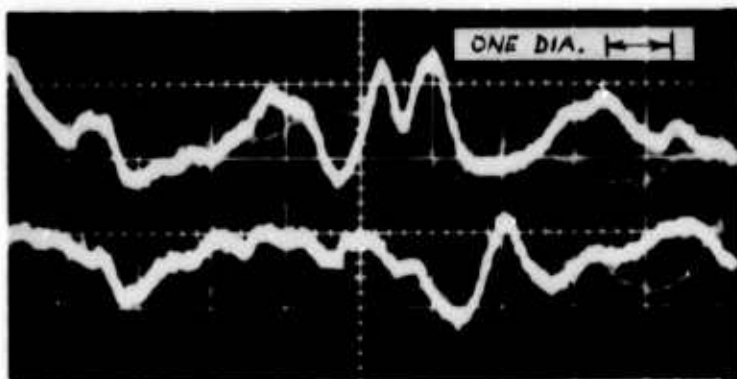N = 12.75; Sweep = 0.1 sec/cm

24
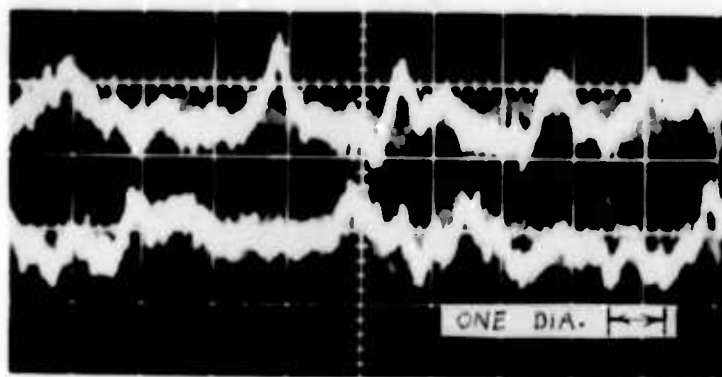
Rey = 1240
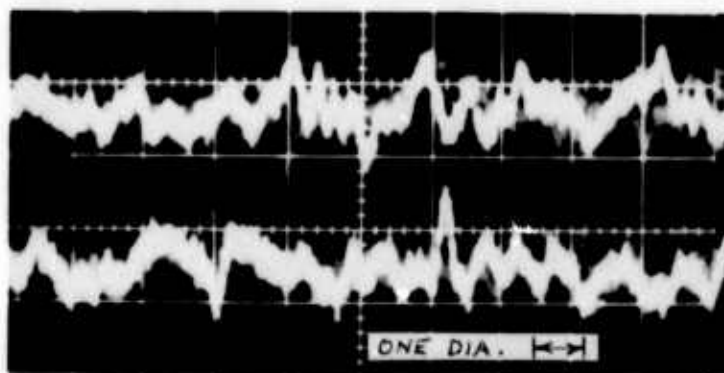
Rey = 1330

Rey = 1540

Fig. 17   Fluctuations Between Rod Probes
N = 12.75; Sweep = 0.1 sec/cm; Amplitude = 1 mv/cm

25

Rey = 1780
N = 12.75
Sweep = .05 sec/cm
Amplitude = 1 mv/cm
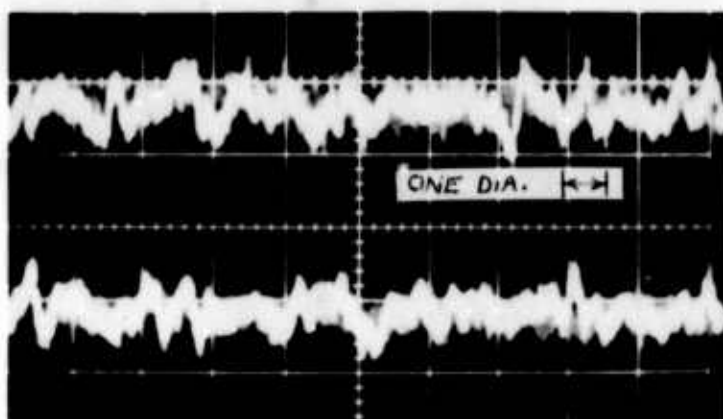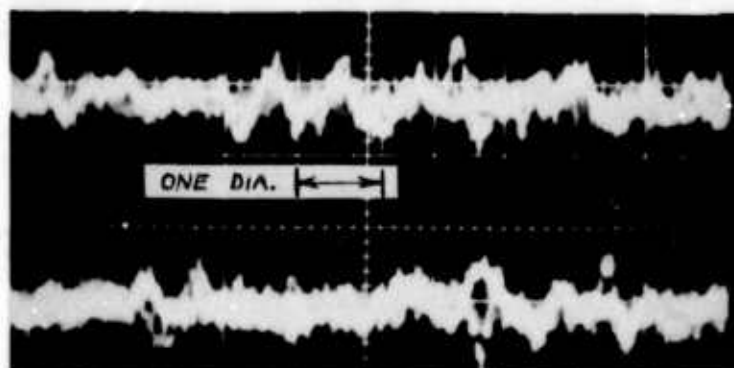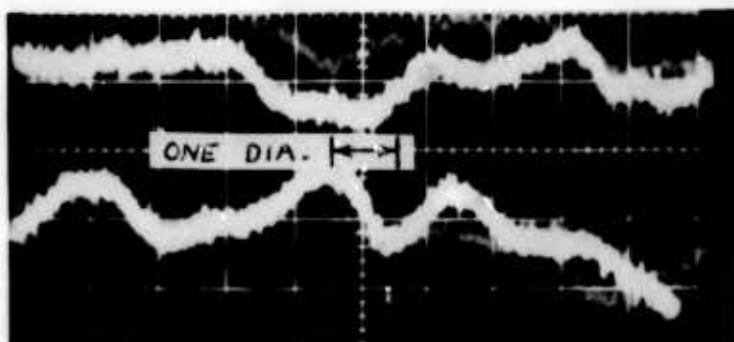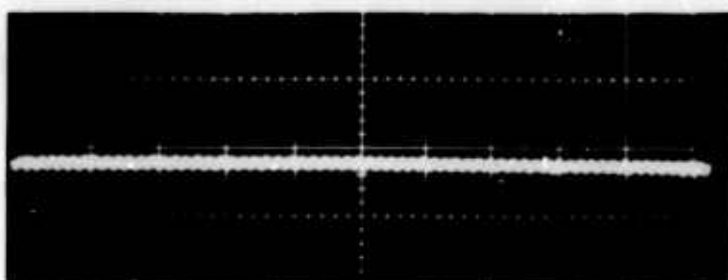
Rey = 0
N = 12.75
Sweep = .1 sec/cm
Amplitude = 1 mv/cm

Rey = 0
N = 0
Sweep = .1 sec/cm
Amplitude = .5 mv/cm

Fig. 18   Fluctuations Between Rod Probes

the presence of the probes induces a true turbulence in the region near the probes which is reflected in a high-frequency component to the observed disturbances; yet transition to turbulence in the major portion of the pipe has not occurred.

The last photograph on Fig. 18 shows the trace for no flow and no corona current to give, as a matter of reference, the background noise level.

Since the disturbance patterns were observed to be combinations of many wavelengths, a harmonic analysis was performed with the aid of a computer. Figures 19 and 20 show the traces which were analyzed and the results of the analysis. The wavelengths listed correspond to the length of a disturbance moving down the pipe at a velocity equal to the mean velocity of the axial flow. The relative magnitudes of certain wavelengths present in the trace are listed. The results indicate that the main disturbances have a characteristic length of about 2, 3, or 4 times the pipe diameter.

Of course since the disturbances are measured by two stationary probes a fixed distance of $\frac{1}{2}$-inch part, the relative magnitudes of various wavelengths will be distorted when measured by the probes.

2. Detection of a Critical Charge Number

If the occurrence of secondary flow is truly caused by a destabilization of the primary flow, a critical value of the destabilizing electric parameter would be expected to exist, below which the primary flow is stable. The ion current effect on the friction factor, and the disturbances measured on the probes should therefore theoretically not appear until a finite value of current density is exceeded. The critical current density may also depend on the Reynolds number.

An attempt to detect a critical charge number was performed as follows:

A constant axial flow Reynolds number of 1150 was obtained in the pipe. With the two rod probes connected to the oscilloscope, the disturbance pattern was observed as the ion current was increased. At the same time, the static pressure drop in the pipe between points 45 inches and 127 inches from the upstream end were measured. The resulting oscilloscope traces are shown in Fig. 21. A very slight periodicity is seen to appear at the fourth trace, at a charge number of 3.52; at higher charge numbers the distrubance pattern is more obvious. Below N = 3.52 a wave pattern is not observed, however, it is realized that the waves may be present at small amplitude. The existence of the relatively large amplitude of high-frequency corona oscillations in this range makes the detection of onset difficult.

Figure 22 shows the friction factors measured as a function of charge number in this range. A definite increase in the friction
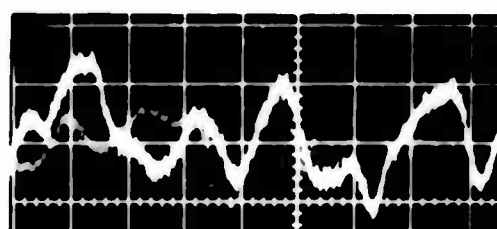
N = 12.85
Rey = 786
Sweep = .1 sec/cm
Amplitude = 1 mv/cm

Wavelength (inches)	Relative Magnitude (Maximum = 1.0)
10.6	.75
5.3	.60
3.5	.96
2.6	1.0
2.1	.41
1.8	.57
1.5	.36
1.3	.32
1.2	.37
1.1	.19

Fig. 19 Harmonic Analysis of Oscilloscope Trace
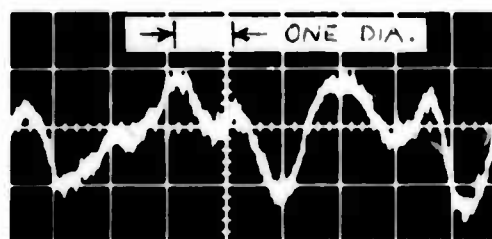
N = 12.85
Rey = 931
Sweep = .1 sec/cm
Amplitude = 1 mv/cm

Wavelength (inches)	Relative Magnitude (Maximum = 1.0)
12.7	.68
6.3	1.0
4.2	.92
3.2	.20
2.5	.85
2.1	.72
1.8	.57
1.6	.20
1.4	.07
1.3	.09

Fig. 20   Harmonic Analysis of Oscilloscope Trace

N = 0

N = 1.72

N = 2.78

N = 3.52

N = 4.45

N = 5.3

N = 6.07

N = 6.65

N = 7.58

Fig. 21   Fluctuations Between Rod Probes at Constant
Reynolds Number of 1150

Sweep = .1 sec/cm;   Amplitude = .5 mv/cm

Fig. 22 Friction Factor Times Reynolds Number Versus Charge Number

31

factor is observed, and the trend is to be a linear fraction of the charge number. If the line at the higher charge numbers is extrapolated to the value of the friction factor at zero charge number, the charge number at this point represents the 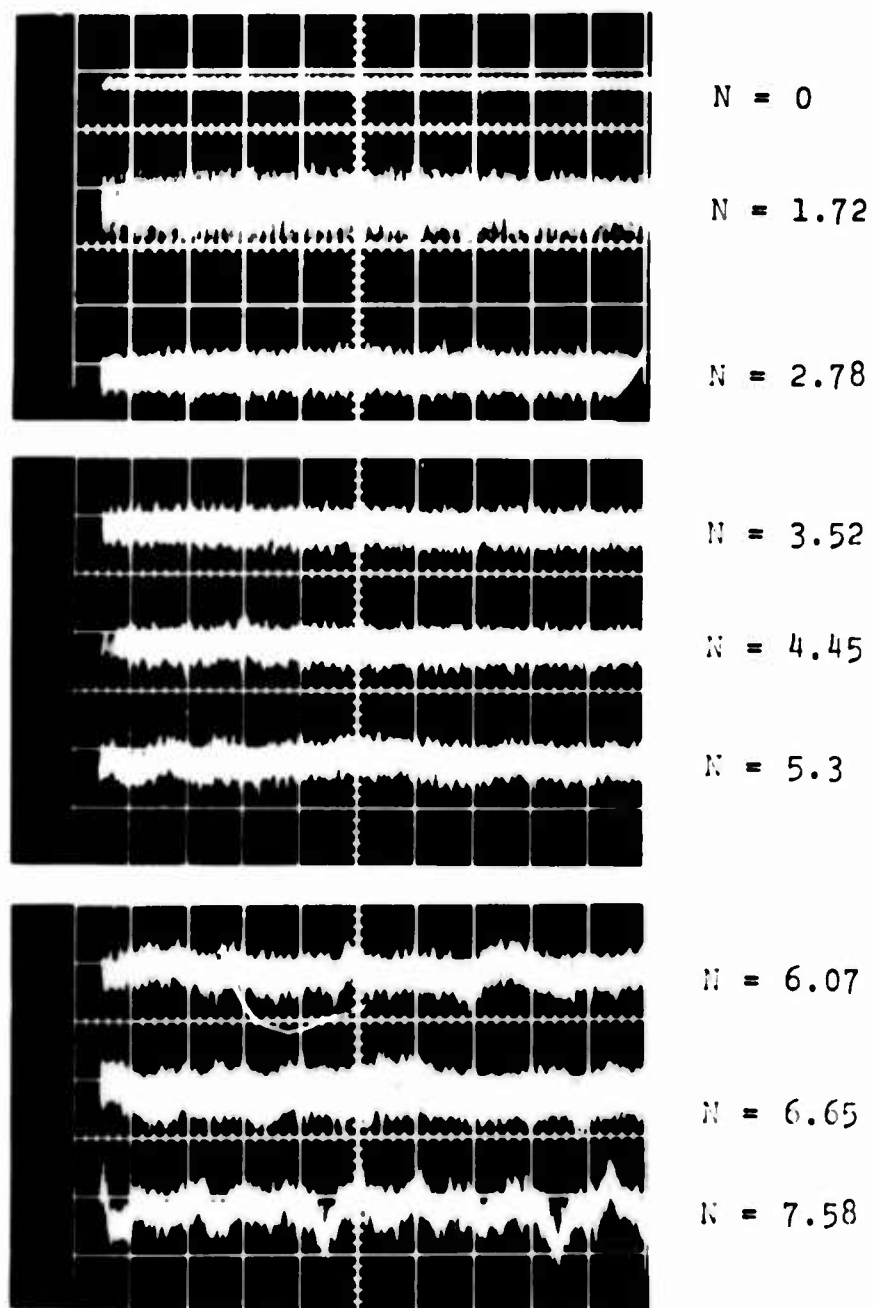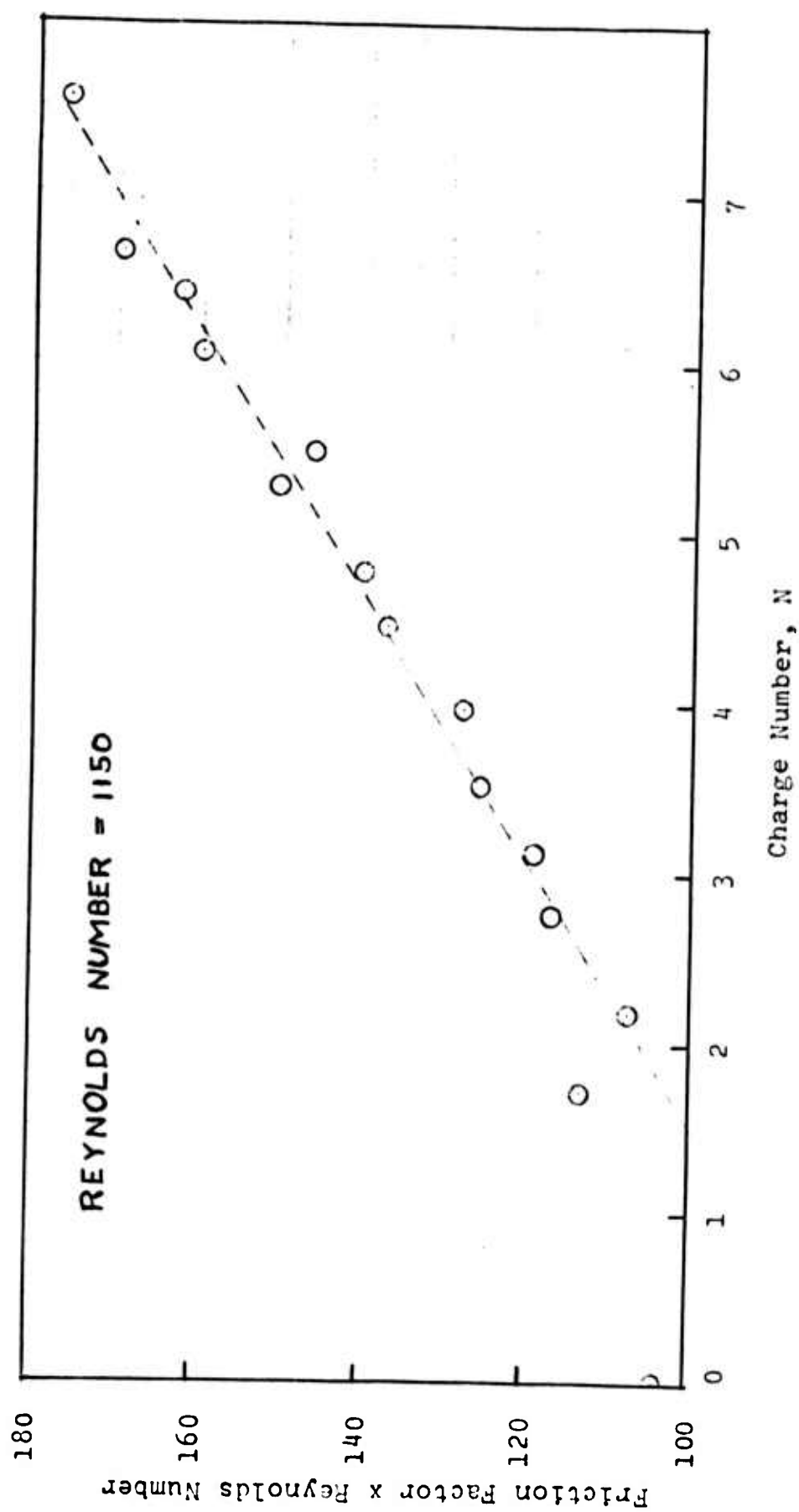critical charge number, or onset of electric effect on the friction factor. The dashed line on Fig. 22 shows this point to be at a charge number of 1.8, corresponding to a current density of 1.52 μA/inch^2 of pipe.

The detection of a critical current is a difficult experimental task. At very low current densities in the pipe the current distribution along the pipe tends to become nonuniform because of slight changes in geometry along the pipe. The measurement of the friction factor over a relatively long length of pipe may then conceivably include sections of pipe which are above critical current and sections where the current is below critical. The above method of using probes to detect secondary flow is similar in principle to a method used by Donnelly[7] to detect vortices between concentric cylinders. In the present case, however, the probe method is made difficult because the ion drift velocity is very large compared to the velocities characteristic of secondary flows.

3. Ring Probes

Disturbances were also measured by having two of the ring probes connected to the oscilloscope. The extreme downstream ring (ring no. 1) and the eight ring were used as probes; the probe separation distance was therefore 0.68 inch. Figures 23 and 24 show the observed disturbance patterns at a constant charge number of 18.3 for several different Reynolds numbers. Again at zero Reynolds number a low-frequency oscillation is seen to be present. At finite Reynolds numbers the disturbance patterns again reveal characteristic wavelengths. The length indicated on the photographs indicates the distance corresponding to a wavelength of one pipe diameter, based on the mean axial flow velocity as before. Several traces, such as the next to the last one on Fig. 23 and 24 indicate that the main disturbance has a wavelength approximately twice the pipe diameter. In any case, the results do indicate that characteristic wavelengths are indeed present.

The amplitudes of the disturbances were a maximum for the traces at Rey = 900, and decreased at higher Reynolds numbers, in agreement with the trend observed with the rod probes. The amount of decrease with the ring probes was less, however. Another difference in the observed traces with the two sets of probes is the type of disturbances at high Reynolds numbers. Beginning at around Rey = 1300, the disturbances with the rod probes began to contain a high-frequency component; this phenomenon was not observed with the ring probes. It is not known at this time whether this difference is caused by the disturbing effect of the rod probes themselves, or the true disturbance patterns at different pipe radii.

Figure 25 shows similar traces, but at a constant Reynolds number and increasing charge number. The lowest charge number indicated

32

Rey = 0
Sweep = .05 sec/cm

Rey = 0
Sweep = .02 sec/cm
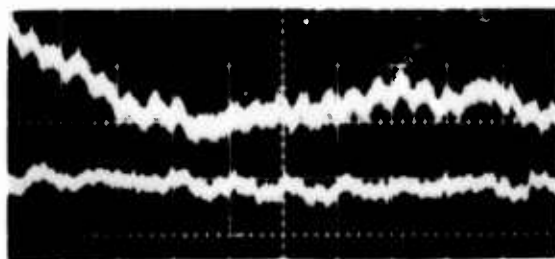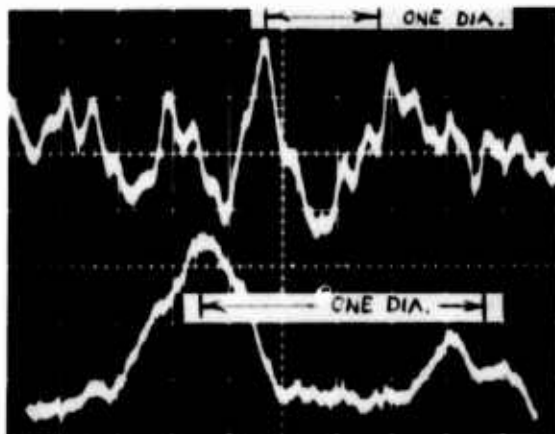
Rey = 900
Sweep = .05 sec/cm

Rey = 900
Sweep = .02 sec/cm
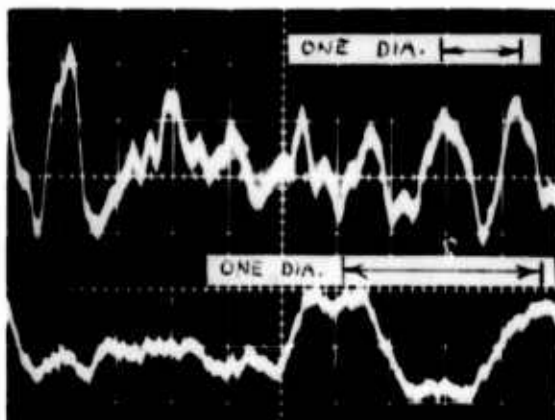
Rey = 1320
Sweep = .05 sec/cm

Rey = 1320
Sweep = .02 sec/cm

Fig. 23   Fluctuations Between Ring Probes

N = 18.3;   Amplitude = 5 mv/cm
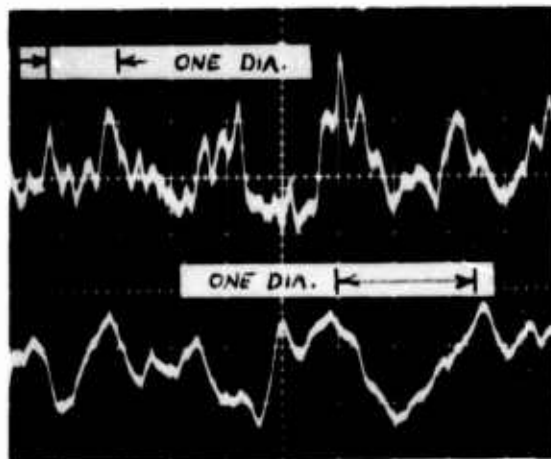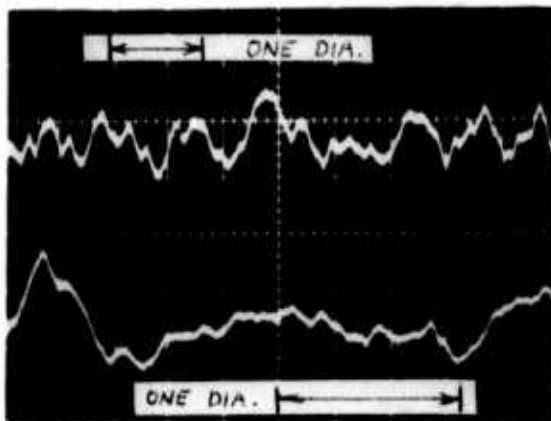
33

Rey = 3750
Sweep = .02 sec/cm

Rey = 3750
Sweep = .01 sec/cm

Rey = 5620
Sweep = .01 sec/cm

Rey = 5620
Sweep = .005 sec/cm

Fig. 24   Fluctuations Between Ring Probes

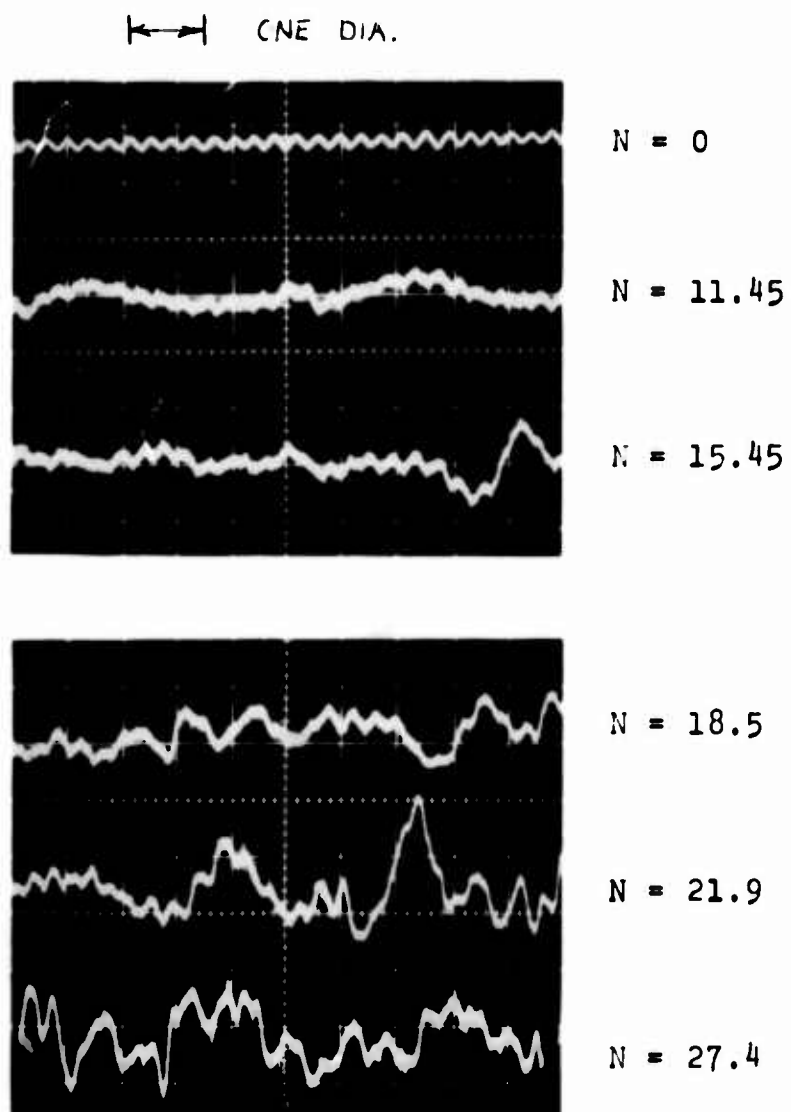N = 18.3;   Amplitude = 5 mv/cm

Fig. 25   Fluctuations Between Ring Probes

Rey = 1400;   Amplitude = 10 mv/cm;   Sweep = .05 sec/cm

a characteristic wavelength of about four diameters; at higher charge numbers wavelengths of the order of one diameter are discernable in the traces.

MEASUREMENT OF STATIONARY DISTURBANCES

Toroidal-shaped, electrically induced vortices are postulated to be generated in the pipe at a Reynolds number of zero. When the primary flow consists of an axial motion this secondary flow would combine with the Poiseuille primary flow in a complicated way. It would be advantageous then to be able to measure the secondary flow when the Reynolds number is zero. To achieve this end, part of the current from a ring was passed through a resistor before being grounded, and the resulting voltage drop across the resistor was placed across the terminals of an oscilloscope. A mechanically driven rotary switch successively connected each ring to the resistor, so that the net effect over one revolution of the switch was to indicate on the oscilloscope the relative variation of current in the rings (see rotary switch circuit, Fig. 26). The rotary switch turned one revolution every 1.35 seconds. A variable amount of current, due to secondary flow, would hopefully be reflected in a disturbance pattern on the oscilloscope.

Figures 27-28 show the resulting oscilloscope traces. Within the range of the moving probe, a peak on the traces is observed, suggestive of a characteristic wavelength on the order of two pipe diameters. This measurement has the drawback that the scanned portion of the pipe is less than one wavelength. If an axial flow is present when the rotating switch is operating, the resulting traces are as shown in Fig. 29. This case is a combination of a moving and stationary probe, where the characteristic velocity would be the sum of the mean air velocity and the effective velocity of the moving ring probe.

Since the rotary switch was limited to contacting 23 variable ring probes, a longer portion of the pipe could be scanned by the following method. Every odd-numbered ring was connected to the rotary switch while every even-numbered ring was grounded. In this way a total length of 2.93 inches of the pipe was scanned by the moving probe. Figure 30 shows the traces observed for several charg numbers. When the rotating contact is between two contacts, the oscilloscope beam moves to the zero position (upward in the photographs); the traces, therefore, appear as a nearly vertical lines, the terminals of which represent the measured quantity. The traces on Fig. 30 show that almost one complete wavelength of about 2.8 inches, or very nearly two pipe diameters, is present. Figure 31 shows a similar series of photographs but in this case the oscilloscope was fixed with a low-persistance screen; as a result the only visible trace appears when the electron beam dwells for an instant before moving to the zero position. These points show some scatter, but again almost a complete wavelength corresponding to about two pipe diameters is observed.
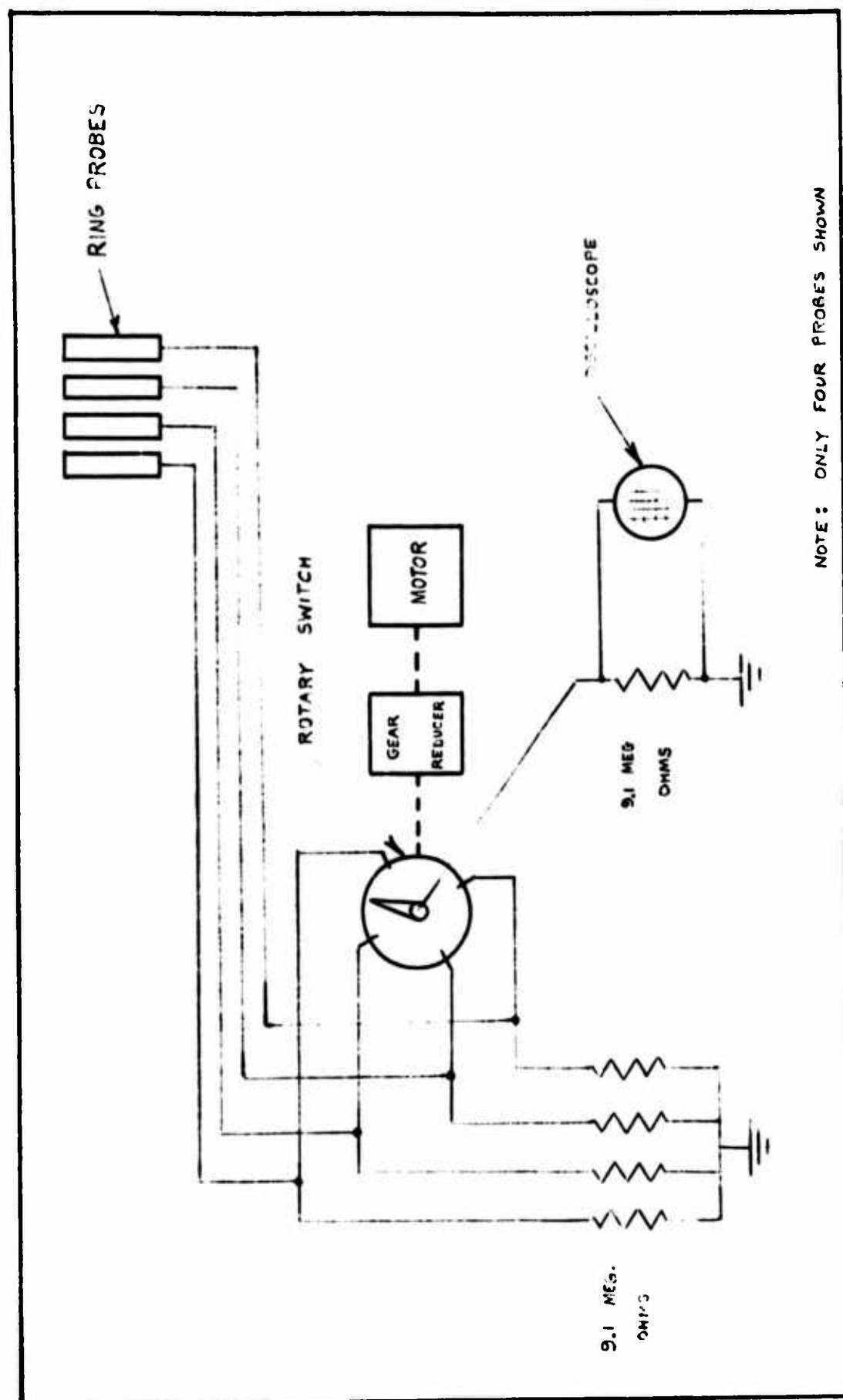
Fig. 26 Rotary Switch Circuit

N = 0
Amplitude = 5 mv/cm
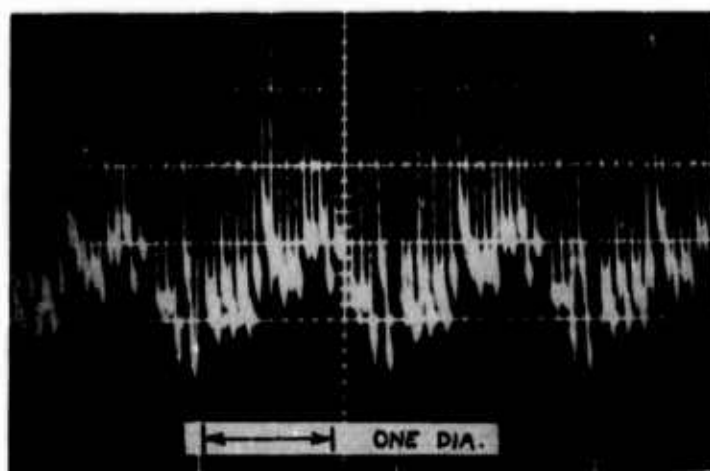
N = 10.83
Amplitude = 20 mv/cm

Fig. 27   Fluctuations on Moving Ring Probe

Rey = 0;   Sweep = .5 sec/cm

N = 14.7
Amplitude = 20 mv/cm
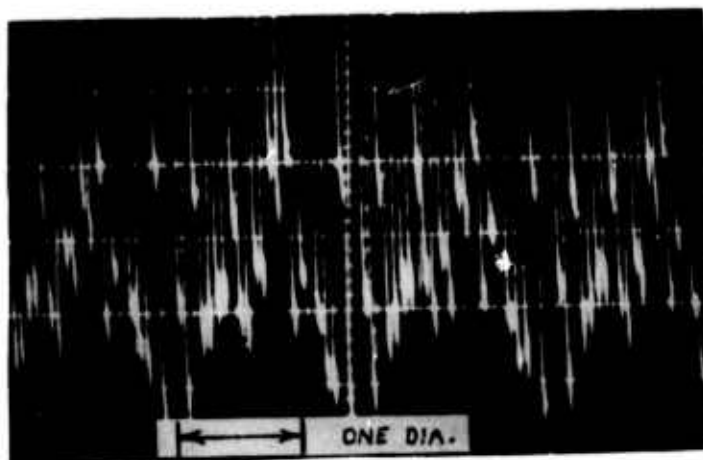
N = 21.2
Amplitude = 20 mv/cm

Fig. 28   Fluctuations on Moving Ring Probe

Rey = 0;   Sweep = .5 sec/cm

39

Rey = 971

Rey = 2800
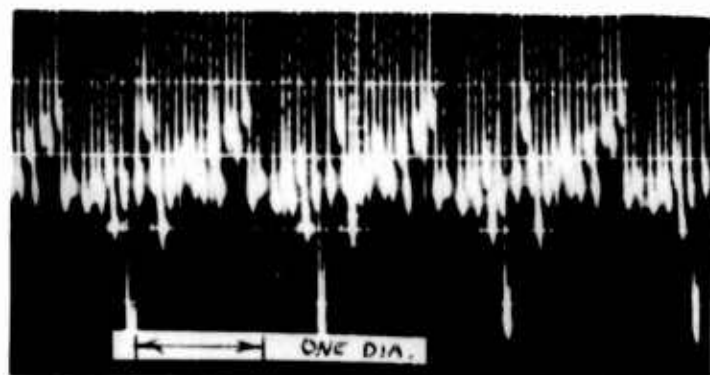
Rey = 7160

Fig. 29   Fluctuations on Moving Ring Probe

N = 1^4;   Sweep = .5 sec/cm;   Amplitude = 20 mv/cm

N = 8.4
Amplitude = .2 mv/cm
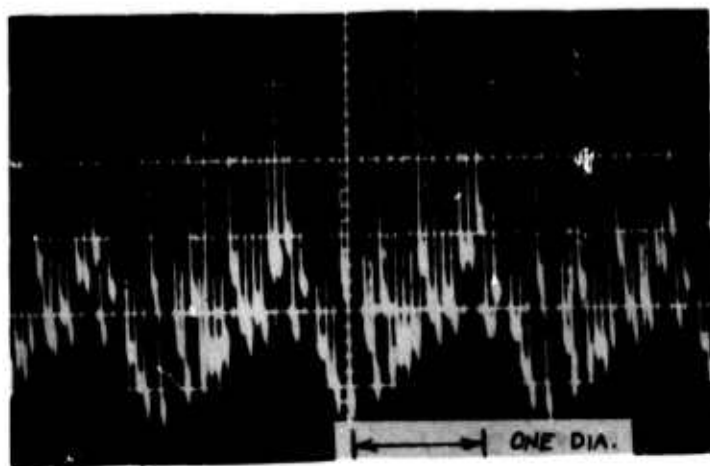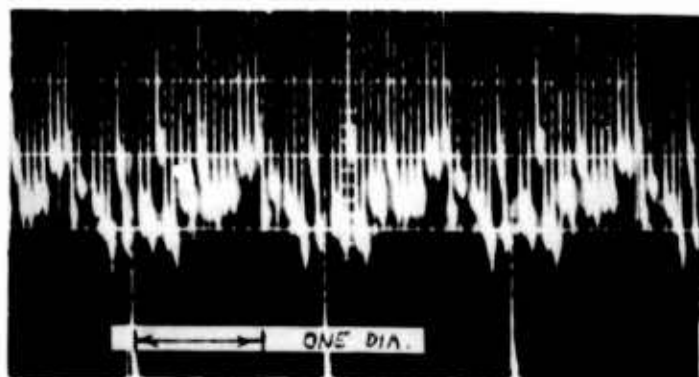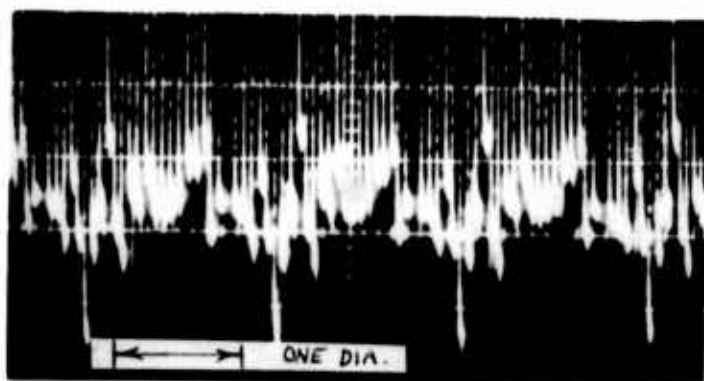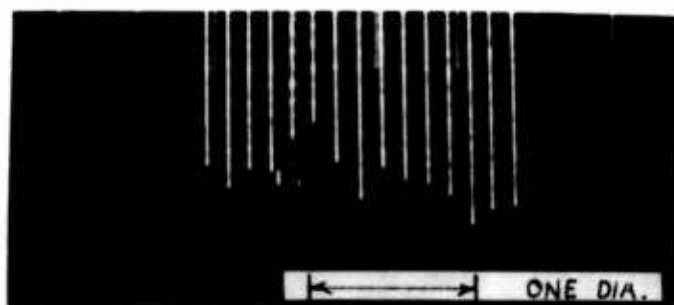
N = 13.4
Amplitude = .5 mv/cm
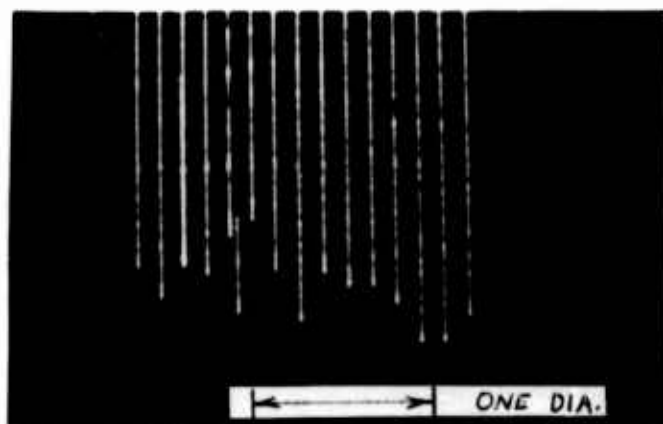
N = 16.2
Amplitude = .5 mv/cm

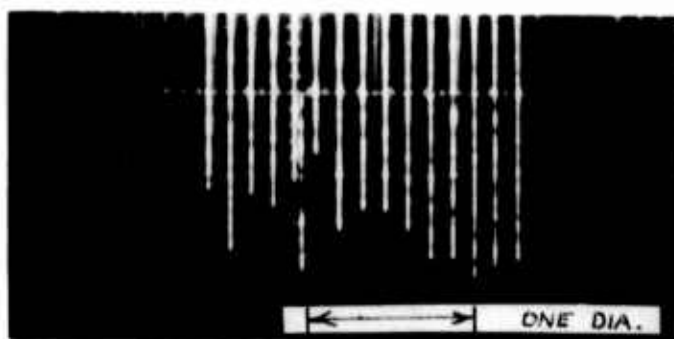Fig. 30   Fluctuations on Moving Ring Probe

Rey = 0;   Sweep = .2 sec/cm

41

N = 13.1

N = 16.0

N = 19.1

Fig. 31   Fluctuations on Moving Ring Probe

Rey = 0;   Amplitude = 20 mv/cm;   Sweep = .2 sec/cm

SUMMARY

The electrostatic probe technique used in this investigation showed that local disturbances in the electric field were present in the pipe. These disturbances were postulated to be caused by coupling of an electrically induced vortex motion with the ion current. In axial flow, such induced vortex motion would be expected to considerably affect the momentum transport within the pipe, in agreement with the experimental observations of the increase in friction factor. From the wavelength of the disturbances, there were indications that the secondary flows had a characteristic length of about two pipe diameters when no axial flow was present, and that several characteristic lengths were super-imposed when there was axial flow.

A determination of the local ion density at a point within and at the wall of the pipe using the probes gave substantial agreement with the theoretical one-dimensional equations. No effect on the local ion density was measurable as the axial flow Reynolds number was increased from 0 up to a value of over 5000.

The results of the present investigation give support to the concept of an electric destabilization of flow in a pipe as proposed in Ref. 4. Since the interaction of the secondary flow with the primary flow is quite large, it is recommended that the analysis be extended to cover additional geometrical and electrical configurations.

43

REFERENCES

1. O'Hara, J. C., "The Effect of a Radial Electric Field on the Flow of a Non-Conducting Gas in a Circular Duct," Ph.D. Thesis, The Ohio State University, 1963.

2. Velkoff, H. R., "An Analysis of the Effect of Ionization on the Laminar Flow of a Dense Gas in a Channel," RTD-TDR-63-4009, Aero Propulsion Laboratory, Air Force Systems Command, Wright-Patterson Air Force Base, Ohio (October, 1963).

3. Pejack, E. R., and Velkoff, H. R., "The Effect of Transverse Ion Current on the Flow of Air in a Flat Duct," U. S. Army Research Office - Durham, Contract No. DA-31-124-ARO-D-246, Technical Report No. 2 (February, 1967).

4. Chuang, T., and Velkoff, H. R., "Analytical Studies of the Effects of Ionization on Fluid Flows," U. S. Army Research Office - Durham, Contract No. DA-31-124-ARO-D-246, Technical Report No. 6 (June, 1967).

5. Cobine, J. D., Gaseous Conductors, Dover Publications, New York, N. Y. (1958).

6. Schlichting, H., Boundary Layer Theory, McGraw-Hill Book Co. New York, N. Y. (1960), p. 439.

7. Donnelly, R. J., "Experiments on the Stability of Viscous Flow between Rotating Cylinders: IV. The Ion Technique," Proceedings of the Royal Society, A, Vol. 283 (1965), pp. 509-519.

DOCUMENT CONTROL DATA · R&D

(Security classification of title, body of abstract and indexing annotation must be entered when the overall report is classified)

1. ORIGINATING ACTIVITY *(Corporate author)*	2a. REPORT SECURITY CLASSIFICATION
The Ohio State University Research Foundation 1314 Kinear Road Columbus, Ohio 43212	Unclassified
	2b. GROUP

3. REPORT TITLE

THE DETECTION OF ELECTRICALLY-INDUCED SECONDARY FLOWS IN A PIPE BY MEANS OF ELECTROSTATIC PROBES

4. DESCRIPTIVE NOTES *(Type of report and inclusive dates)*

Interim Technical Report

5. AUTHOR(S) *(Last name, first name, initial)*

Velkoff, Henry R., and Pejack, Edwin R.

6. REPORT DATE	7a. TOTAL NO. OF PAGES	7b. NO. OF REFS
August, 1967	51	7

8a. CONTRACT OR GRANT NO. DA-31-124-ARO-D-246	9a. ORIGINATOR'S REPORT NUMBER(S)
b. PROJECT NO. 20010501B700	Technical Report # 7
c. 1D12140A142	9b. OTHER REPORT NO(S) *(Any other numbers that may be assigned this report)*
d.	

10. AVAILABILITY/LIMITATION NOTICES

Distribution of this document is unlimited

11. SUPPLEMENTARY NOTES	12. SPONSORING MILITARY ACTIVITY U. S. Army Research Office - Durham Box CM, Duke Station Durham, North Carolina 27706

13. ABSTRACT

An experimental investigation was conducted to detect the presence of electrically induced secondary flows inside a round pipe. A thin concentric wire in the pipe was impressed with a high positive voltage which generated a corona discharge, producing ions and a radial electric field in the pipe. It was postulated that secondary flows taking the form of vortex flows inside the pipe would result.

A technique of utilizing electrostatic probes inserted into the pipe and on the wall provided strong evidence that secondary flows were generated both with and without a primary axial flow. At zero axial flow the characteristic length of the secondary flow was on the order of two pipe diameters. With an axial flow, when the primary and secondary flows are superimposed, various characteristic lengths were observed.

DD FORM 1473
1 JAN 64

14. KEY WORDS	LINK A		LINK B		LINK C	
	ROLE	WT	ROLE	WT	ROLE	WT
Electro Fluidmechanics						
Corona Discharge						
Induced Vortex						

INSTRUCTIONS

1. ORIGINATING ACTIVITY: Enter the name and address of the contractor, subcontractor, grantee, Department of Defense activity or other organization (*corporate author*) issuing the report.

2a. REPORT SECURITY CLASSIFICATION: Enter the overall security classification of the report. Indicate whether "Restricted Data" is included. Marking is to be in accordance with appropriate security regulations.

2b. GROUP: Automatic downgrading is specified in DoD Directive 5200.10 and Armed Forces Industrial Manual. Enter the group number. Also, when applicable, show that optional markings have been used for Group 3 and Group 4 as authorized.

3. REPORT TITLE: Enter the complete report title in all capital letters. Titles in all cases should be unclassified. If a meaningful title cannot be selected without classification, show title classification in all capitals in parenthesis immediately following the title.

4. DESCRIPTIVE NOTES: If appropriate, enter the type of report, e.g., interim, progress, summary, annual, or final. Give the inclusive dates when a specific reporting period is covered.

5. AUTHOR(S): Enter the name(s) of author(s) as shown on or in the report. Enter last name, first name, middle initial. If military, show rank and branch of service. The name of the principal author is an absolute minimum requirement.

6. REPORT DATE: Enter the date of the report as day, month, year; or month, year. If more than one date appears on the report, use date of publication.

7a. TOTAL NUMBER OF PAGES: The total page count should follow normal pagination procedures, i.e., enter the number of pages containing information.

7b. NUMBER OF REFERENCES: Enter the total number of references cited in the report.

8a. CONTRACT OR GRANT NUMBER: If appropriate, enter the applicable number of the contract or grant under which the report was written.

8b, 8c, & 8d. PROJECT NUMBER: Enter the appropriate military department identification, such as project number, subproject number, system numbers, task number, etc.

9a. ORIGINATOR'S REPORT NUMBER(S): Enter the official report number by which the document will be identified and controlled by the originating activity. This number must be unique to this report.

9b. OTHER REPORT NUMBER(S): If the report has been assigned any other report numbers (*either by the originator or by the sponsor*), also enter this number(s).

10. AVAILABILITY/LIMITATION NOTICES: Enter any limitations on further dissemination of the report, other than those imposed by security classification, using standard statements such as:

  (1) "Qualified requesters may obtain copies of this report from DDC."

  (2) "Foreign announcement and dissemination of this report by DDC is not authorized."

  (3) "U. S. Government agencies may obtain copies of this report directly from DDC. Other qualified DDC users shall request through

    _____ ."

  (4) "U. S. military agencies may obtain copies of this report directly from DDC. Other qualified users shall request through

    _____ ."

  (5) "All distribution of this report is controlled. Qualified DDC users shall request through

    _____ ."

If the report has been furnished to the Office of Technical Services, Department of Commerce, for sale to the public, indicate this fact and enter the price, if known.

11. SUPPLEMENTARY NOTES: Use for additional explanatory notes.

12. SPONSORING MILITARY ACTIVITY: Enter the name of the departmental project office or laboratory sponsoring (*paying for*) the research and development. Include address.

13. ABSTRACT: Enter an abstract giving a brief and factual summary of the document indicative of the report, even though it may also appear elsewhere in the body of the technical report. If additional space is required, a continuation sheet shall be attached.

It is highly desirable that the abstract of classified reports be unclassified. Each paragraph of the abstract shall end with an indication of the military security classification of the information in the paragraph, represented as *(TS)*, *(S)*, *(C)*, or *(U)*.

There is no limitation on the length of the abstract. However, the suggested length is from 150 to 225 words.

14. KEY WORDS: Key words are technically meaningful terms or short phrases that characterize a report and may be used as index entries for cataloging the report. Key words must be selected so that no security classification is required. Identifiers, such as equipment model designation, trade name, military project code name, geographic location, may be used as key words but will be followed by an indication of technical context. The assignment of links, rules, and weights is optional.